JOURNAL OF QUATERNARY SCIENCE (2025) 1–18 ISSN 0267-8179. DOI: 10.1002/jqs.70006

JQS Journal of Quaternary Science QRA Quaternary Research Association

A tephrostratigraphic investigation of the continuously varved Holocene Boreal lake Nautajärvi, Finland, provides precise age estimate for Lairg A/Hekla 5 eruption

ALICE CARTER-CHAMPION,[1,2]* KATY FLOWERS,[1] ANTTI E.K. OJALA,[3,4] SIMON BLOCKLEY,[1] PAUL LINCOLN,[1] SHUANG ZHANG,[1] CHRISTINA MANNING[5] and CELIA MARTIN PUERTAS[1]

[1]Department of Geography, Centre of Quaternary Research, Royal Holloway, University of London, Egham, TW20 0EX, UK
[2]Department of Geography, University College London, University of London, London, WC1E 6BT, UK
[3]Department of Geography and Geology, University of Turku, Turku, FI-20014, Finland
[4]Geological Survey of Finland, Espoo, FI-02151, Finland
[5]Department of Earth Science, Centre for Dynamic Earth and the Solar System, Royal Holloway, University of London, Egham, TW20 0EX, UK

Received 24 February 2025; Revised 24 July 2025; Accepted 28 July 2025

ABSTRACT: Numerous cryptotephra layers originating from Icelandic volcanoes and further afield have reached Northern Europe during the Holocene. Refining the precise timing and the relative frequency of local and distal eruptions requires well-resolved continuous sediment archives. Lake Nautajärvi is located in central-southern Finland (61°48′ N, 24°41′ E), and contains a continuous sequence of 9898 varves. Nautajärvi was isolated from the Baltic Sea basin at the Lake Ancylus phase ~9600 varve yr BP. We present a tephrostratigraphic record of Nautajärvi for targeted intervals within the Holocene, aiming to identify tephra from the largest eruptions, to enable an alignment with other varved lakes in Northern Europe containing tephra layers, like Diss Mere, Tiefer See and Meerfelder Maar. Geochemical analyses were produced for 26 peaks in tephra concentration, with five cryptotephra deposits corresponding to known eruptions from the mid and late Holocene. The far-travelled KS_2 eruption from Ksudach caldera in Kamchatka is identified, enabling an alignment to Greenland, which is strengthened by the identification of the Hekla 4 tephra in Nautajärvi. Close to the KS_2 deposition in Nautajärvi, a Hekla-type eruption correlating to the Lairg A/Hekla 5 is also identified—macroscale counting of the varves between the KS_2 and Lairg A layers enables a constrained age estimate (7001 ± 44 Cal yr BP) of the Lairg A eruption to be made. The widespread Glen Garry tephra was also identified within the Nautajärvi sequence, with an age estimate of 2088 ± 21 varve yr BP. Finally, there is also a tentative correlation to the Suduroy tephra, with an older age estimate than from the sites in which it was originally identified (8459 ± 84 varve yr BP). The remaining layers correspond to eruptions from more distal sources—several chemistries may correlate to mid-Holocene eruptions from North America (Mount Rainier, Aniakchak, Katmai), with one shard tentatively associated with Azorean chemistry. This record provides well-constrained age estimates for two key Holocene tephras (Glen Garry, Lairg A) and highlights the potential for far-travelled tephras from North America and Kamchatka to reach Northern Europe, emphasising the benefits of further tephra studies in Scandinavia. © 2025 The Author(s). *Journal of Quaternary Science* Published by John Wiley & Sons Ltd.

KEYWORDS: chronology; Holocene; tephrochronology; tephrostratigraphy; varves

Introduction

Tephrochronology offers the opportunity to precisely align and synchronise chronologies across multiple palaeoenvironmental records, to effectively assess the differences and propagation of past climate changes across regions (Lowe, 2011; Davies, 2015). It has been widely applied across Europe in Holocene peat records (Wastegård, 2002; Pilcher et al., 2005; Watson et al., 2016), with ~100 tephra layers identified thus far from source areas as distal as North America, Kamchatka and Mexico (Plunkett and Pilcher, 2018; Kalliokoski et al., 2023). As these peat records often contain low sedimentation rates and limited independent chronological constraints, there may be substantial age uncertainties associated with the Holocene cryptotephras thus far identified within Europe. Supplementing these are several annually resolved varved sediment records, located in Central and Northern Europe, which contain better constrained age estimates that can enable a more precise synchronisation of climate records across Europe (Zillén, Wastegård and Snowball, 2002; Wulf et al., 2016; Kinder et al., 2020; Martin-Puertas et al., 2021). Extending this well-resolved varved network of cryptotephra chronologies (Bronk Ramsey et al., 2015) is crucial for linking high-resolution archives of climatic change and is the key aim of this study.

Lake Nautajärvi is located in southern Finland, in the northeastern sector of the Holocene European tephra lattice, and its sedimentary record is continuously varved from ~9850 varve yr BP to the present day (Ojala and Alenius, 2005). Recent tephrochronological investigations in Finland (Kalliokoski et al., 2019; Kalliokoski et al., 2020; Kalliokoski et al., 2023) have shown that tephra sourced from several regions are deposited in Finland (e.g., Iceland, North America). As Nautajärvi benefits from well-refined existing

*Correspondence: Alice Carter-Champion, as above.
Email: Alice.Carter-Champion@rhul.ac.uk

varve and palaeomagnetic chronologies (Ojala and Tiljander, 2003; Ojala and Alenius, 2005), it should yield a valuable tephrostratigraphic record to critically evaluate previous ages assigned to known tephra and to verify the robustness of the varve record of Nautajärvi. This record will also provide the opportunity in the future to precisely synchronise and compare climate proxy records across Europe.

The aim of this paper is, thus, to target known widespread eruptions that have already been identified in other annually resolved records (Diss Mere, Tiefer See and Greenland ice cores) for several key intervals in the early, mid and late Holocene. The oldest target interval will aim to identify tephra from the Hekla–Torfajökull complex between ~8200 and 6600 Cal a BP (Walsh et al., 2021, 2023), while the Hekla 4 tephra (4325 ± 8 Cal BP) (Davies et al., 2024) will be the focus of the second target interval. Finally, the Glen Garry tephra will be targeted at ~2100 Cal a BP (Barber et al., 2008), as this tephra is also widespread across northern Europe. To account for possible offsets in the varve chronology, wider intervals will be targeted, to maximise the likelihood of identifying the target tephra (Table 1).

Study site

Nautajärvi (61°46′ N, 24°24′ E, 103.7 m asl) is a 20 m deep dimictic lake, sitting within a series of hydrologically linked lakes in south-central Finland (Fig. 1). There are three inflows to the lake from the NE (partially derived from Ristijärvi), north and NW, with one southerly outflow draining into lake Pitkävesi. Nautajärvi was formed during the Early Holocene following recession of the Fennoscandian Ice Sheet at ~11 000 Cal a BP and isolation from the Baltic Sea basin during the Lake Ancylus interval, at ~9625 varve yr BP (Ojala et al., 2005). At the time of deglaciation, the highest shoreline in the Nautajärvi area was at c. 155 m a.s.l. and the lake was part of the ancient Baltic Sea basin for about 1400 years prior to isolation (Supporting Information S1: Fig. 1). The silt and clay deposits that cover ca. 25% of the current lake Nautajärvi catchment were deposited during this period, first in a proglacial environment and then in more glacier distal settings. These fine-grained deposits appear in lower lying areas and have since been eroded by inflowing ditches and minor rivers into the Nautajärvi basin. The broader catchment geology is granitic in nature, and is partially covered by glacial till with some peat deposits. There are surficial coarse and fine sand deposits from relic glacial features, in addition to finer clay–silt materials. Presently, the lake is ice-covered for <5 months per year, with the spring snowmelt discharge into Nautajärvi providing the clastic component of the clastic-biogenic varves: the organic layer is deposited in the summer months and is composed of fine particulate and amorphous organic material (Ojala and Alenius, 2005; Ojala et al., 2013; Korkonen et al., 2017).

Methods

Nautajärvi was first cored in 1999 using a piston corer and has a well-established independently verified chronology (Ojala

Table 1. Summary of tephra peaks identified within each target interval for the Nautajärvi sediment sequence in this study, with age estimates, shard concentrations and proposed volcanic sources included.

Target interval	Initial sampling resolution	Cryptotephra sample	Composite depth (cm)	Varve chronology (varve yr BP (Ojala and Alenius, 2005)	Shard concentration (s/g)	Volcanic source(s)	Majors?
Glen Garry: 1680–2268 Cal a BP	2-cm	NAU_T119	119	1798 ± 18	22	—	N
		NAU_T124	124	1878 ± 18	18	Katla, Aniakchak?	Y (5)
		NAU_T139.5	139	2088 ± 21	18	Askja, Torfajökull, Katmai?	Y (11)
Hekla 4: 3909–4800 Cal a BP	2-cm	NAU_T255	255	4145 ± 41	338	Hekla, Katla, unknown	Y (19)
		NAU_T266	266	4333 ± 43	6	Katla	Y (2)
		NAU_T276	276.5	4507 ± 45	44	Katla	Y (2)
		NAU_T281	281	4578 ± 46	17	Askja?	Y (1)
Hekla–Torfajökull complex: 6290–8580 Cal a BP	1-cm	NAU_T396	396	6395 ± 64	69	Katla	Y (4)
		NAU_T405	405	6532 ± 65	28	Katla	Y (2)
		NAU_T410.5	410.5	6631 ± 66	19	Katla, Rainier	Y (7)
		NAU_T416	416	6726 ± 67	24	Hekla, Katla, Rainier	Y (5)
		NAU_T418	418	6762 ± 68	595	Hekla	Y (15)
		NAU_T422	422	6827 ± 68	74	Ksudach	Y (23)
		NAU_T426	426	6897 ± 69	42	Katla, Furnas	Y (3)
		NAU_T430	430	6966 ± 70	5	—	N
		NAU_T441	441	7149 ± 71	15	—	N
		NAU_T454	454	7327 ± 73	46	Katla	Y (4)
		NAU_T461.5	461.5	7443 ± 74	21	Katla	Y (1)
		NAU_ T476	476	7678 ± 77	33	Katla	Y (3)
		NAU_T482	482	7780 ± 78	27	Katla, unknown	Y (8)
		NAU_T486	486	7830 ± 78	30	Katla	Y (4)
		NAU_T496	496	7999 ± 80	27	Katla	Y (6)
		NAU_T500	500	8041 ± 80	24	Katla, Hekla?	Y (5)
		NAU_T503	503	8084 ± 81	14	Katla	Y (3)
		NAU_T506	506	8128 ± 81	13	—	N
		NAU_T511.5	511	8204 ± 82	12	Katla	Y (3)
		NAU_T518	518	8283 ± 83	12	—	N
		NAU_T525	525	8377 ± 84	12	Katla	Y (1)
		NAU_T532	532	8459 ± 85	102	Katla	Y (27)
		NAU_T538	538	8533 ± 85	16	Katla	Y (2)
		NAU_T540	540	8556 ± 86	15	Katla	Y (1)

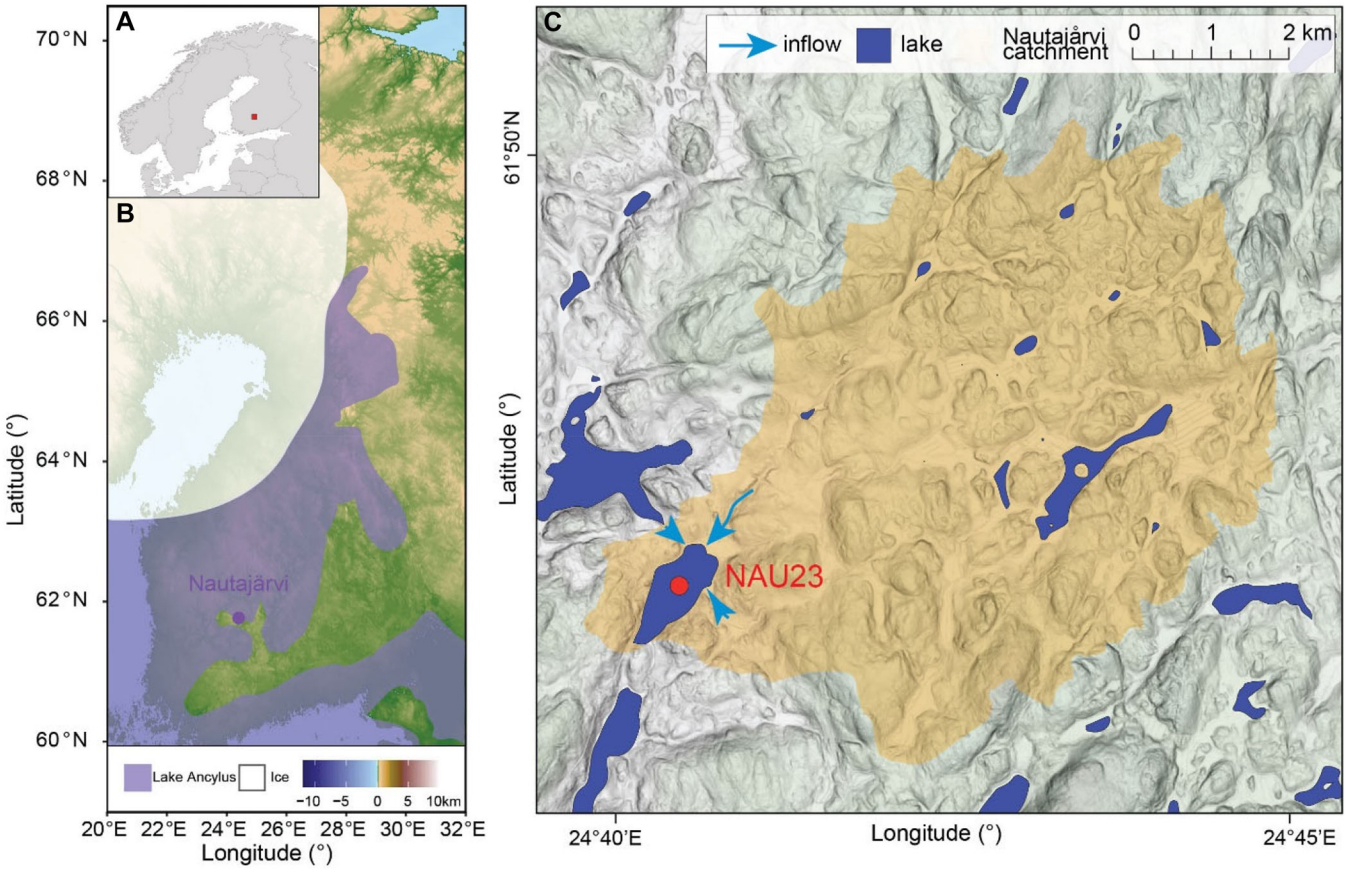

Figure 1. Location of Nautajärvi lake within the broader European context. (A) The red box denotes the location of the site. (B) Previous Early Holocene extent of the lake Ancylus and supra-aquatic areas of early-Holocene Finland, redrawn from Andrén et al. (2011). Nautajärvi occurs close to the margin of such an early Holocene lake. (C) More detailed catchment context of Nautajärvi. [Color figure can be viewed at wileyonlinelibrary.com]

and Alenius, 2005; Ojala et al., 2005, 2008). This is primarily based on annual-layer counting from the semi-automated software DendroScan and verified by high-resolution X-ray images, in addition to palaeomagnetic secular variation analysis, which provides the independent component of the precision of this chronology (Ojala and Tiljander, 2003). Varve yr BP is determined as the varve years before CE 1950, as previously presented for Nautajärvi varve counting chronology (Ojala and Saarinen, 2002; Tiljander et al., 2002; Ojala and Alenius, 2005).

In 2023, new sediment cores were collected from Nautajärvi to construct a targeted tephrostratigraphy and to analyse for additional proxies, detailed in Lincoln et al. (2025). These cores were collected from the deepest part of the lake, using a gravity piston corer from the frozen lake in March 2023, with four core sequences retrieved (10 drives in total) within 10 m of each other. This allowed for clear overlaps between the different drives and cores were cut into sections of varying lengths. The new cores were correlated to the existing records and published varve chronology at the macroscale, using the 210 distinct marker layers appearing at 5–20 cm intervals and identified in all present and previously cored sediment sequences (Ojala and Alenius, 2005; Lincoln et al., 2025). This was then verified using the originally cored X-ray images matched to high-resolution XRF data obtained on the 2023 sequence (Lincoln et al., 2025).

The tephra sampling strategy was designed to identify the key tephra horizons already identified in varved European sequences like Diss Mere (Walsh et al., 2021, 2023) and Tiefer See (Dräger et al., 2017). As the Nautajärvi chronology is high precision (1% counting error—(Ojala and Alenius, 2005)), we analysed contiguous 2-cm or 1-cm samples within an interval corresponding to the known varve age of a tephra (including uncertainties) following procedures described for tephra investigation in varved sediments (Walsh et al., 2023). A total of 217 samples were taken and dried, then combusted at 105°C overnight and then at 550°C for 4 h, to also obtain a coarse measure of percentage organic content (Loss-on-ignition; Heiri et al. (2001)). Carbonates were removed via the addition of 10% HCl for 30 min and samples were sieved at 15 μm: after initial tests, it became evident that an additional sieving stage at 125 μm was not required. Cryptotephra extraction was then performed using the technique of Turney (1998), with amendments from Blockley et al. (2005). Extracted material was mounted in Canada balsam and counted using high-powered polarising light microscopy. Shard concentrations were calculated as a proportion of the total dried weight of sediment and peaks were identified visually using the shard depth profile outlined in Fig. 2.

Samples containing significant peaks in tephra above background concentrations were selected for major element geochemical analysis at 1-cm resolution, with individual grains picked and analysed on carbon-coated stubs using the Cameca SX-100 electron microprobe analyser (EPMA) at the Tephra Analysis Unit in the University of Edinburgh (TAU). This system uses an accelerating 15 keV voltage and a series of beam currents for different elements, ranging from 0.5 nA to 60 nA (Hayward, 2012). The beam size for major element analysis was 3 μm to account for the small shards with variable morphologies. Internal standards (Lipari and BCR-2G) were analysed at the start and end of each analysis day to ensure that the geochemistry can be well calibrated. A 95% analytical total cut-off value was used for all analyses.

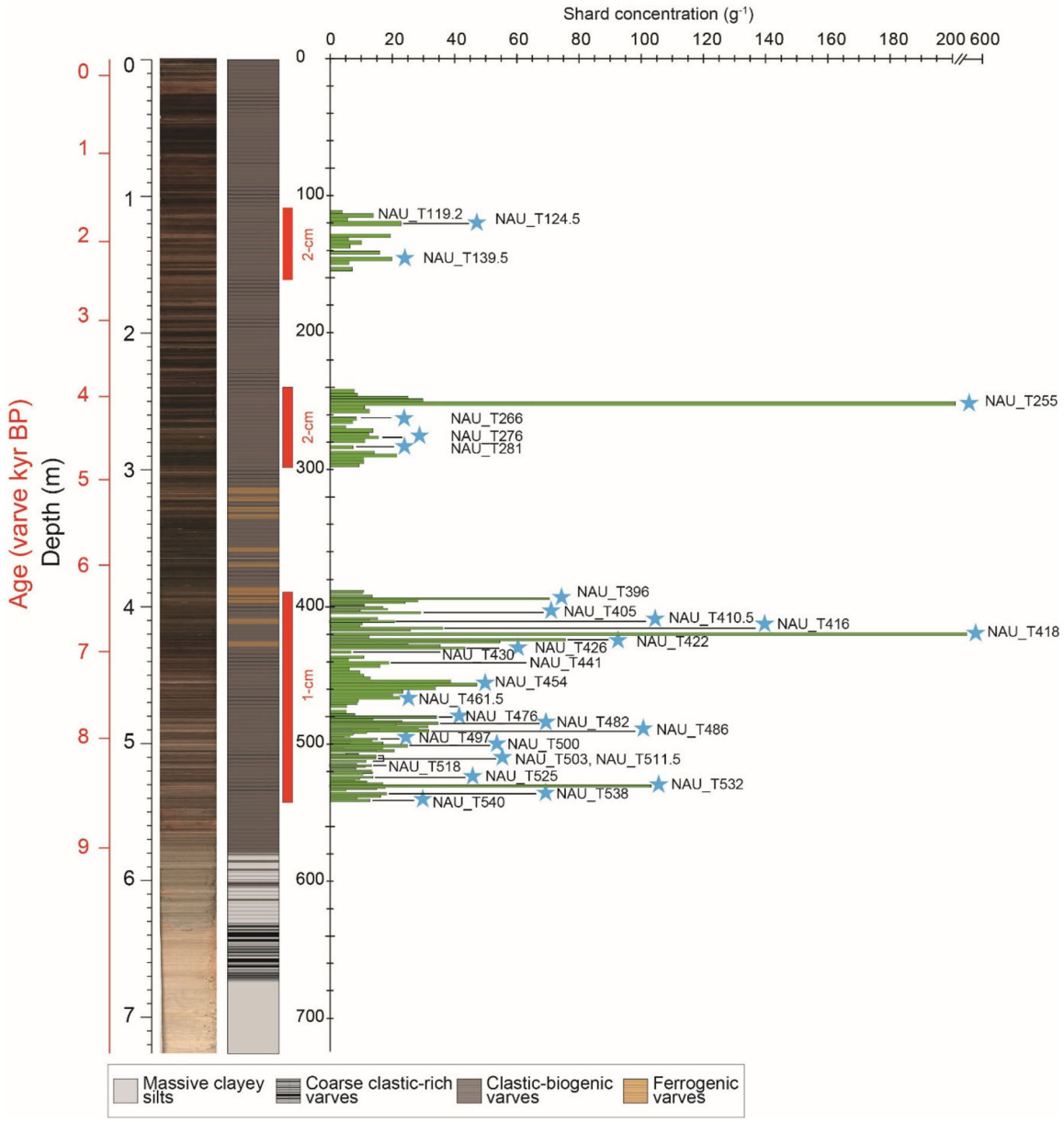

Figure 2. NAU-23 profile showing the key sedimentological changes and core photos, alongside the target intervals scanned for tephra (red bars) and the shard concentrations at 1 or 2 cm resolution. Blue stars denote where the sample was geochemically analysed, with the key target intervals focussing on locating the Glen Garry, Hekla 5 and Hekla 5–Torfajökull complex of the early-mid Holocene. [Color figure can be viewed at wileyonlinelibrary.com]

Trace element geochemistry was also acquired for one cryptotephra sample using the Laser Ablation-Inductively Coupled Plasma-Mass Spectrometer in the department of Earth Science at Royal Holloway, University of London. An Agilent 8900 ICP-MS was coupled to a Resonetics ArF eximer laser ablation system (Müller et al., 2009) with a machine set up for tephra analysis following the methods of Tomlinson et al. (2010). Between samples, the standards NIST 610 and NIST612 and MPI-DING standards ATHO-G, StHs-80 and Gor-128 were analysed as internal and secondary calibration standards, respectively. Shards were ablated for 40 s at 5 Hz with a 15 µm spot size. Mapping from major elements ensured that normalised ^{29}Si values from Wavelength Dispersive Spectroscopy-EPMA were processed with each shard, so normalisation could occur in post-analysis processing alongside the internal calibration of NIST 612. Tephra geochemistry was plotted and analysed in R using the AshplotR repository (Matthews and Pike, 2022), with amendments for trace elements and greater plotting flexibility. All major and trace element compositions along with glass standard data are presented in the Supporting Information S2.

In order to assess the impact of the tephra age estimates on the overall varve chronology, as well as the variation in the local reservoir effect within Nautajärvi over the Holocene, several Bayesian age models were created. Radiocarbon dates from Ojala et al. (2019) were calibrated and a site-specific reservoir correction was used in several *P_Sequence* deposition models in Oxcal v4.4 with different *K* factors (Bronk Ramsey, 2008; Ramsey, 2009; Ramsey and Lee, 2013). Three deposition models were developed for NAU-23; the first used only the bulk ^{14}C dates presented in Ojala et al. (2019), with a constant reservoir correction (630 yrs) calculated from the offset between an Intcal20 calibrated date that is coincident with the Glen Garry tephra in NAU-23, alongside a variable *K* factor (Reimer et al., 2020). The second model uses the relative varve ages as the *z* value within the model with a fixed *K* value and the independent tephra-age estimates, similar to the approach used in the construction of the Diss Mere age model (Martin-Puertas et al., 2021). Finally, a more flexible approach was used, with a variable *K* factor and the tephra ages, to account for potential offsets between the varve age

estimates and the independent tephra age estimates. In all models, Bayesian outlier detection was used at 95% confidence using the 'general model' in Oxcal.

Results and interpretation

For the three target intervals identified for this study (Glen Garry, Hekla 4 and the early Holocene Hekla–Torfajökull complex), 31 cryptotephra peaks were identified in the Nautajärvi sequence, which does not cover the entire record (see Fig. 2 for shard concentrations and the composite tephrostratigraphy). As several of these tephra peaks are small, geochemical analyses could only be obtained for 26 of these layers, with a limited number of analyses (<5) for 13 of these peaks. In most cases, geochemical analyses with minor populations ($n < 2$) are not discussed, but can be found in the Supporting Information S1. Based on major-element geochemistry, only five of these layers can be correlated to known eruptions (Table 2). Five further eruptions with chemical affinities to known volcanic systems have also been identified, with tentative correlations to source proposed in the Supporting Information S2. Eruptions came from four Icelandic volcanic systems, with one deposit from the Cascades, two from the Alaskan–Aleutian arc region and one correlating to the Kamchatkan volcanic region. There is also one tentative correlation to the Azorean volcano Furnas, although the precise eruption is currently unconstrained. The geochemical results and potential correlations are presented below, divided into the target intervals.

Target interval 1: Hekla–Torfajökull complex (389–542 cm; 6290–8600 varve yr BP)

The shard concentration profile of this interval (Fig. 2) contains a substantial amount of tephra shards—which occur in the Nautajärvi samples both in terms of constant flux (<15 shards/g) of background signal and as several distinct peaks of up to 700 shards/g. There are 18 peaks for the interval 6800–8600 varve yr BP (NAU_T426–NAU_T540; Table 1) that show mainly homogeneous geochemistry across and within all peaks: all but two outliers (from NAU_T426 and NAU_T500) contain SiO_2 content of 71–72 wt.%, 3.7–4 wt.% FeO and 5.3–5.7 wt.% Na_2O. This geochemical distribution is consistent with the Katla-type chemistry from southern Iceland (the rhyolitic component; Na_2O ranges of 4.9–5.6 wt.% and 3.4–4.2 wt.% FeO), which has been well correlated across the North Atlantic region, and is associated with the Vedde Ash eruption of Katla at ~12 100 Cal a BP (Lane et al., 2012). A more recent eruption of Katla (the Suduroy tephra) has been identified in the Faroe islands (Wastegård, 2002) and Norway (Pilcher et al., 2005), dated to 7860–8310 Cal a BP (Wastegård, 2002), which corresponds fairly well to the suite of Katla layers analysed in the Nautajärvi sequence. Based on the shard peaks, the peak of 102 shards/g at NAU_T532 (8459 ± 85 varve yr BP) could correspond with the Suduroy tephra, although the Nautajärvi varve age range is older than the maximum age from the Faroe Islands by almost 200 years. This peak, although the highest concentration, is not the first input of rhyolitic Katla-type shards identified in the Nautajärvi tephrostratigraphy. There are several smaller peaks lower in the stratigraphy between 532 and 540 cm (NAU_T538 and NAU_T540 respectively) with Katla-type chemistry. This may suggest that either there was a preceding Early Holocene Katla eruption that has not been thus far recognised from western European tephra records, or that the majority of this Katla-type chemistry at Nautajärvi is derived from some secondary input from the surrounding catchment. This hypothesis is considered further in the discussion.

The non-Katla chemistry identified from NAU_T426 is trachytic in nature with high K_2O values (5.46 wt.%), matching eruptive products from the Azorean volcanic system of Furnas

Table 2. Average values of key tephra layers identified in this study.

Sample	*n*		SiO_2	TiO_2	Al_2O_3	FeO	MnO	MgO	CaO	Na_2O	K_2O	P_2O_5	Total
NAU_T124.5 pop 1	3	Wt.%	70.9	0.3	13.3	3.6	0.1	0.2	1.2	5.1	3.4	0.0	98.3
		Sd.	0.9	0.0	0.8	0.2	0.0	0.0	0.1	0.7	0.2	0.0	1.7
		Norm.	72.2	0.3	13.6	3.7	0.1	0.2	1.2	5.2	3.5	0.0	
		Sd.	0.6	0.0	0.6	0.2	0.0	0.0	0.1	0.6	0.2	0.0	
NAU_T139.5 pop 1	8	Wt.%	69.85	0.78	12.31	5.17	0.10	0.80	3.16	4.02	1.77	0.20	98.17
		Sd.	1.68	0.22	0.47	0.93	0.02	0.31	0.63	0.34	0.16	0.09	1.23
Glen Garry		Norm.	71.16	0.79	12.54	5.26	0.10	0.81	3.21	4.10	1.80	0.21	
		Sd.	2.15	0.22	0.38	0.91	0.02	0.31	0.61	0.33	0.17	0.09	
NAU_T255 pop 1	11	Wt.%	59.76	1.17	14.96	9.76	0.24	1.74	5.22	4.44	1.58	0.57	98.57
Andesite		Sd.	0.57	0.03	0.75	0.35	0.02	0.09	0.18	0.37	0.10	0.02	0.77
Hekla 4		Norm.	60.63	1.19	15.18	9.90	0.25	1.76	5.30	4.50	1.60	0.58	
		Sd.	0.41	0.03	0.68	0.39	0.02	0.09	0.19	0.37	0.10	0.02	
NAU_T255 pop 1	4	Wt.%	72.89	0.09	13.14	1.81	0.07	0.02	1.29	4.82	3.00	0.01	96.08
Rhyolite		Sd.	0.80	0.01	0.31	0.18	0.01	0.01	0.07	0.27	0.04	0.01	0.61
Hekla 4		Norm.	75.87	0.09	13.67	1.89	0.08	0.02	1.35	5.01	3.13	0.01	
		Sd.	0.66	0.01	0.29	0.19	0.01	0.01	0.08	0.27	0.06	0.01	0.00
NAU_T418	15	Wt.%	74.49	0.08	11.86	1.67	0.05	0.03	1.25	4.41	2.74	0.02	96.60
		Sd.	0.66	0.01	0.37	0.10	0.01	0.01	0.04	0.22	0.08	0.00	0.72
Lairg A/Hekla 5		Norm.	77.11	0.08	12.27	1.73	0.06	0.03	1.29	4.57	2.83	0.02	
		Sd.	0.40	0.01	0.36	0.11	0.01	0.01	0.04	0.23	0.08	0.00	
NAU_T422	23	Wt.%	67.14	0.58	13.91	4.75	0.15	1.12	3.69	5.21	1.20	0.15	97.91
		Sd.	2.51	0.20	1.85	1.55	0.04	0.56	1.06	0.90	0.56	0.06	1.39
KS_2		Norm.	68.60	0.60	14.21	4.84	0.15	1.14	3.76	5.32	1.23	0.16	
		Sd.	2.96	0.20	1.85	1.55	0.04	0.56	1.06	0.94	0.59	0.06	
NAU_T532	27	Wt.%	69.84	0.28	12.83	3.76	0.12	0.21	1.33	5.36	3.52	0.05	97.31
		Sd.	1.22	0.01	0.41	0.14	0.01	0.02	0.06	0.31	0.10	0.01	1.62
Suduroy		Norm.	71.77	0.29	13.18	3.87	0.12	0.22	1.37	5.51	3.62	0.05	
		Sd.	0.39	0.01	0.32	0.13	0.01	0.02	0.06	0.31	0.09	0.01	

(Guest et al., 2015; Johansson et al., 2017; Wastegård et al., 2019). There is no published glass geochemistry from the Middle Furnas Group, which corresponds to eruptions older than the widespread eruption of Fogo volcano, Fogo A (~5500 Cal a BP) post-dating the formation of the main caldera ~30 ka ago (Guest et al., 1999, 2015). However, based on glass chemistry from Furnas layers C, E, F and I (Wastegård et al., 2019), there is clear overlap between the single analysis from NAU_T426 and Furnas glass chemistry (Fig. 4(C), (D)), suggesting that there may have been an eruption from the Middle Furnas Group at ~6897 varve yr BP, which was far travelled enough to reach Nautajärvi. Indeed, Azorean tephra has been recorded in the UK, Sweden and Ireland in the late-Holocene (Chambers et al., 2004; Johansson et al., 2017; Plunkett and Pilcher, 2018; Walsh et al., 2021), further highlighting the potential for Azorean tephra to reach southern Fennoscandia.

Between 6200 and 6800 varve yr BP, six of the highest concentration peaks were processed for geochemical analysis (NAU_T396, NAU_T405, NAU_T410.5, NAU_T416, NAU_T418 and NAU_T422, Table 1); although there were nine discrete peaks of tephra, very low absolute shards numbers prevented further peaks being selected for geochemical analysis. Three peaks (NAU_T418, NAU_T405 and NAU_T396) contain only rhyolitic chemistry, while NAU_T422, NAU_T416 and NAU_T410.5 have analyses spanning the dacite–rhyolite boundary. The four youngest peaks (NAU_T396, NAU_T405, NAU_T410.5 and NAU_T416) all have Katla-type chemistry present within their peaks. NAU_T396 and NAU_T405 have homogenous Katla-type chemistry, while NAU_T410.5 ($n = 7$) and NAU_T416 ($n = 5$) contain secondary populations that straddle the rhyolite–dacite classification (Table 1). These populations are higher in TiO_2 (1–1.15 wt.%) than the contemporaneous chemistry from Icelandic sources (Hekla 5: 0–0.10 wt.% TiO_2, Torfajökull from Diss Mere: 0.19–0.20 wt.% TiO_2).

These high TiO_2 shards match well to North American sources, particularly with mid-Holocene chemistries from Sydney Bog and Thin Ice Pond in NE America, which have been compared to recent eruptions (<2500 Cal a BP) from Mount Rainier (Sisson and Vallance, 2009). There is significant geochemical overlap between Sydney Bog, Thin Ice Pond and the population in NAU_T410.5 (Jensen et al., 2021). There is good evidence for several eruptions of this volcanic system in the mid-Holocene, but limited glass chemistry available for the Rainier eruptions known as Layer D and Layer L, which are dated using radiocarbon to 6000 ^{14}C a BP and 6400 ^{14}C a BP, respectively (Donoghue et al., 2007). Mean values for the volcanic glass from proximal sections plot broadly within the geochemical envelope for population two of NAU_T410.5. NAU_T416 (n = 5) also contains multiple populations, with several similarities to NAU_T410.5, and with one population (n = 2) sourced from Katla. Population two (NAU_T416_pop2) also correlates tentatively with the layers found in Thin Ice Pond and Sydney Bog, assigned to the Mount Rainier volcanic system by Jensen et al. (2021). Finally, there is one shard in NAU_T416 (NAU_T416_pop3) with lower TiO_2 (0.08 wt.%) that sits within the Hekla geochemical envelope based on major elements.

The two deeper layers identified in this mid-Holocene target interval (NAU_T418 and NAU_T422) both have distinct geochemical signatures. NAU_T418 ($n = 17$) contains homogeneous geochemistry matching Hekla-type chemistry. Shards from the major population are low-alkali metal (Na_2O, K_2O) rhyolites, with average SiO_2 values of 76.89 wt.%, FeO at 1.85 wt.%, TiO_2 at 0.09 wt.% and K_2O at 2.88 wt.%, corresponding well to the average values of the Hekla layers from Diss Mere (Walsh et al., 2023) for a similar time interval (Fig. 3(D)). The age estimate of this peak in Nautajärvi of 6762 ± 67 varve yr BP is younger than the age of the Lairg A eruption, which has been associated with the Hekla volcanic system and is dated to ~7050 Cal a BP (Thorarinsson, 1971; Gudmundsdóttir et al., 2016). In Diss Mere, there is a Hekla eruption identified at 7177 ± 39 Cal a BP, which may correspond to Lairg A, although Walsh et al. (2021, 2023) found several intervals of similar Hekla chemistry found before and after the Lairg A. There is another identified Hekla eruption dated to ~6000 Cal a BP, named the Hekla Ö, that bears some similarities to NAU_T418 but is disregarded in this case, as it is distinguishable by higher TiO_2 and Al_2O_3 values (Ruth Gudmundsdóttir et al., 2011; Jónsson et al., 2020). The Hekla 5 has been identified in Finland already, and dated to 7027 ± 134 Cal yr BP, in agreement with existing age estimates of the eruption (Kalliokoski et al., 2023). Based on the chemical match to published Lairg A/Hekla 5 chemistry, NAU_T418 can be assigned to the Lairg A/Hekla 5 eruption. One outlier analysis from this layer corresponds to the Katla-type chemistry of the overlying layers (NAU_T396, NAU_T405, NAU_T410.5).

The peak found at NAU_T422 (n = 25) is homogeneous, bar three outliers. Of these outliers, two analyses correspond to the Katla-type chemistry seen above and one is a high-silica rhyolite with K_2O and Na_2O values of 3.95 wt.% and 4.35 wt.%, respectively. The major population of NAU_T422 spans the dacite–rhyolite classification: it is low-K in nature (average of 1.07 wt.%), and has an unfractionated Rare Earth Element-normalised pattern, which is characteristic of the Ksudach volcano on the Kamchatkan peninsula (Fig. 4(E)). The KS_2 eruption overlaps the compositional range seen in NAU_T422 as well as the age estimate of the sample (Kyle et al., 2011; Ponomareva et al., 2017; Portnyagin et al., 2020). This tephra dispersal was widespread and has been found in Greenland (Davies et al., 2024) and Svalbard (van der Bilt et al., 2017), but has thus far not been found as far south-east as Finland (Kalliokoski et al., 2023). The Greenland Ice Core age estimate (GICC05 b1.95k) for the KS_2 is 7089 ± 26 Cal a BP (Andersen et al., 2006; Davies et al., 2024), which is several hundred years older than the proximal age estimate of 6877–6693 Cal a BP (Ponomareva et al., 2017). In Nautajärvi, this peak is at ~6827 varve yr BP, which matches well with the proximal age estimate, but is 200 years younger than the ice core age of KS_2. Based on the chemical match, NAU_T422 in the Nautajärvi sequence is correlated to the KS_2 eruption.

Target interval 2: Hekla 4 (241–294 cm; 3909–4800 varve yr BP)

The second interval processed for the Nautajärvi tephrostratigraphic investigation focused on locating the eruption of Hekla 4, to enable correlation with both Diss Mere and the Greenland Ice Cores (Walsh et al., 2021; Davies et al., 2024). As with the lowermost target interval, shard concentrations were mainly low (<10 shards/g) and several small peaks were identified (Table 1). The most abundant of these—NAU_T255—yielded concentrations of 204 shards/g and was analysed for major element analysis. There were 22 successful analyses of this layer, but their chemistry was heterogeneous. The largest population ($n = 11$) sits within the andesitic classification, with high FeO of 9%–10.4% and TiO_2 of ~1.2%. The second population ($n = 4$) is rhyolitic and low-alkali, with affinity to the rhyolitic component of the mid-Holocene Hekla volcanic system in Iceland. Indeed, when proximal glass chemistry of the widespread Hekla 4 eruption (Meara et al., 2020) is compared with both populations of NAU_T255, there is a match with the lower silica and rhyolitic

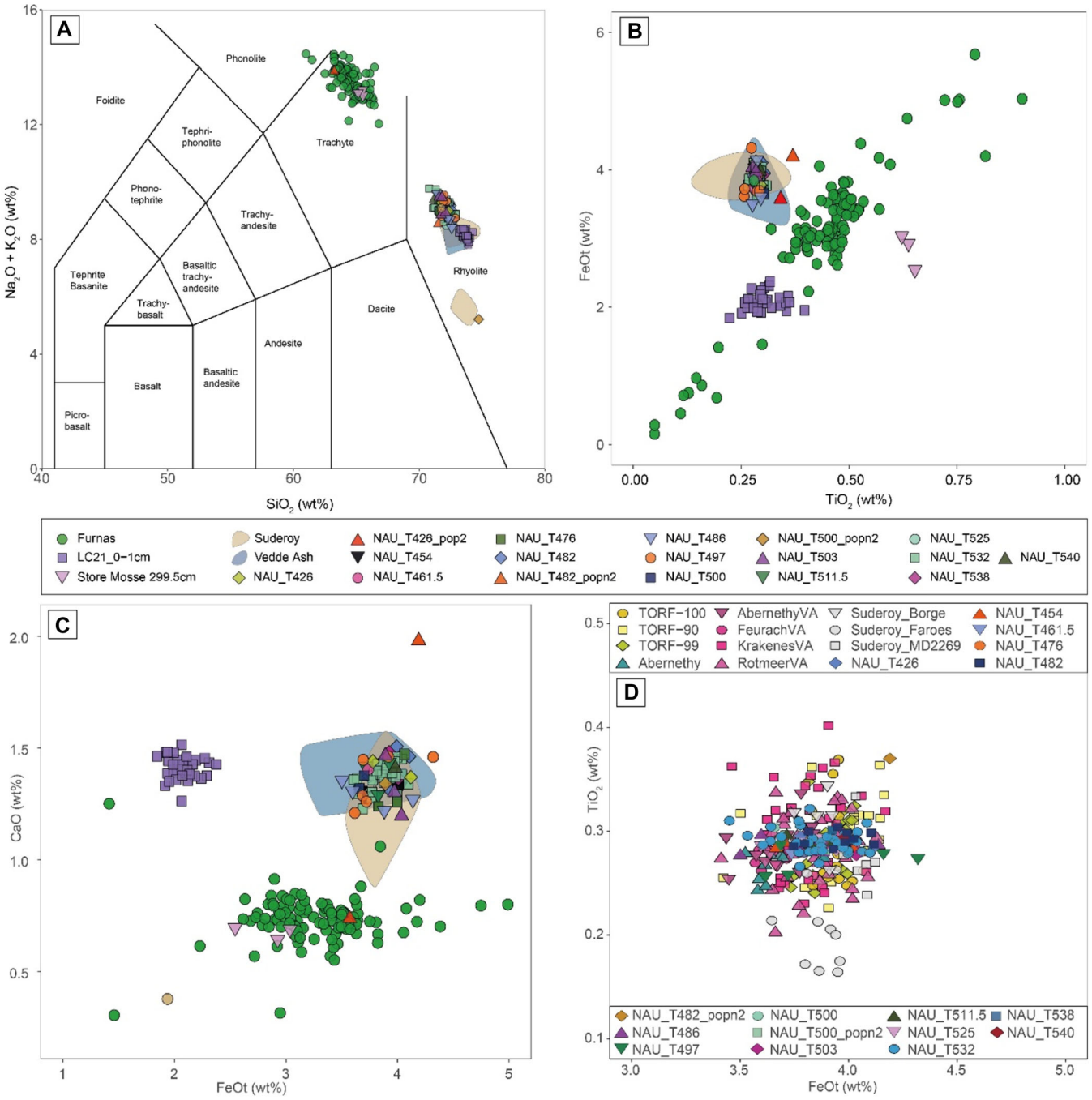

Figure 3. Geochemical analysis of the Early-Holocene tephra layers identified in Nautajärvi. (A) TAS (Bas et al., 1986) plot of the key candidate eruptions plotted alongside NAU_T426—T540. The majority of tephras are medium-high-alkaline rhyolite. For the bi-plots, the data were filtered so that only >60% SiO_2 was plotted for ease of interpretation. (B) FeO–TiO_2 biplot highlighting the spread in both FeO and TiO_2 for the Furnas volcanic system (Guest et al., 2015; Johansson et al., 2017; Wastegård et al., 2019) and the relatively confined Katla-type chemistry. LC21 Santorini chemistry is taken from Satow et al. (2015). (C) FeO–CaO plot indicates the good fit of the trachytic NAU_T426_pop2 with the Furnas volcanic system. (D) FeO–TiO_2 zoomed plot comparing the geochemical distribution of Katla-type chemistry from Torfdalsvatn and several instances of the Vedde Ash and Suduroy tephras (Wastegård, 2002; Pilcher et al., 2005; Kristjánsdóttir et al., 2007) to examine the potential for distinguishing Katla-type chemistry using this bi-plot. There is clear overlap between the NAU Katla-type chemistries and both Torfdalsvatn (Harning et al., 2023) and the published Vedde-type chemistry (Matthews et al., 2011; Lane et al., 2012; Carter-Champion et al., 2022). [Color figure can be viewed at wileyonlinelibrary.com]

components of this eruption (Fig. 5, Supporting Information S1: Fig 2). The varve age 4145 varve yr BP of NAU_T255 also sits close to the published estimates of the widespread Hekla 4 eruption, albeit with some offset, which will be discussed further in the next section. Recently published Hekla 4 chemistry from the Greenland Ice Cores also reveals that lower silica components of this tephra can be found distally, lending confidence to the correlation of NAU_T255 with Hekla 4 in Nautajärvi (Davies et al., 2024). In addition to the Hekla 4 chemistry within NAU_T255, there are two smaller populations. Two analyses of a high-alkali rhyolite correlate on major elements to Katla-type chemistry from the early Holocene, as is seen in the target interval 1. The final population consists of a high-alkali rhyolite with high FeO (5.73%–5.93%) that has not been correlated with a source at present.

Glen Garry target interval (111–150 cm; 1680–2268 varve yr BP)

The uppermost target section in the Nautajärvi sequence contained three cryptotephra peaks, but low shard concentra-

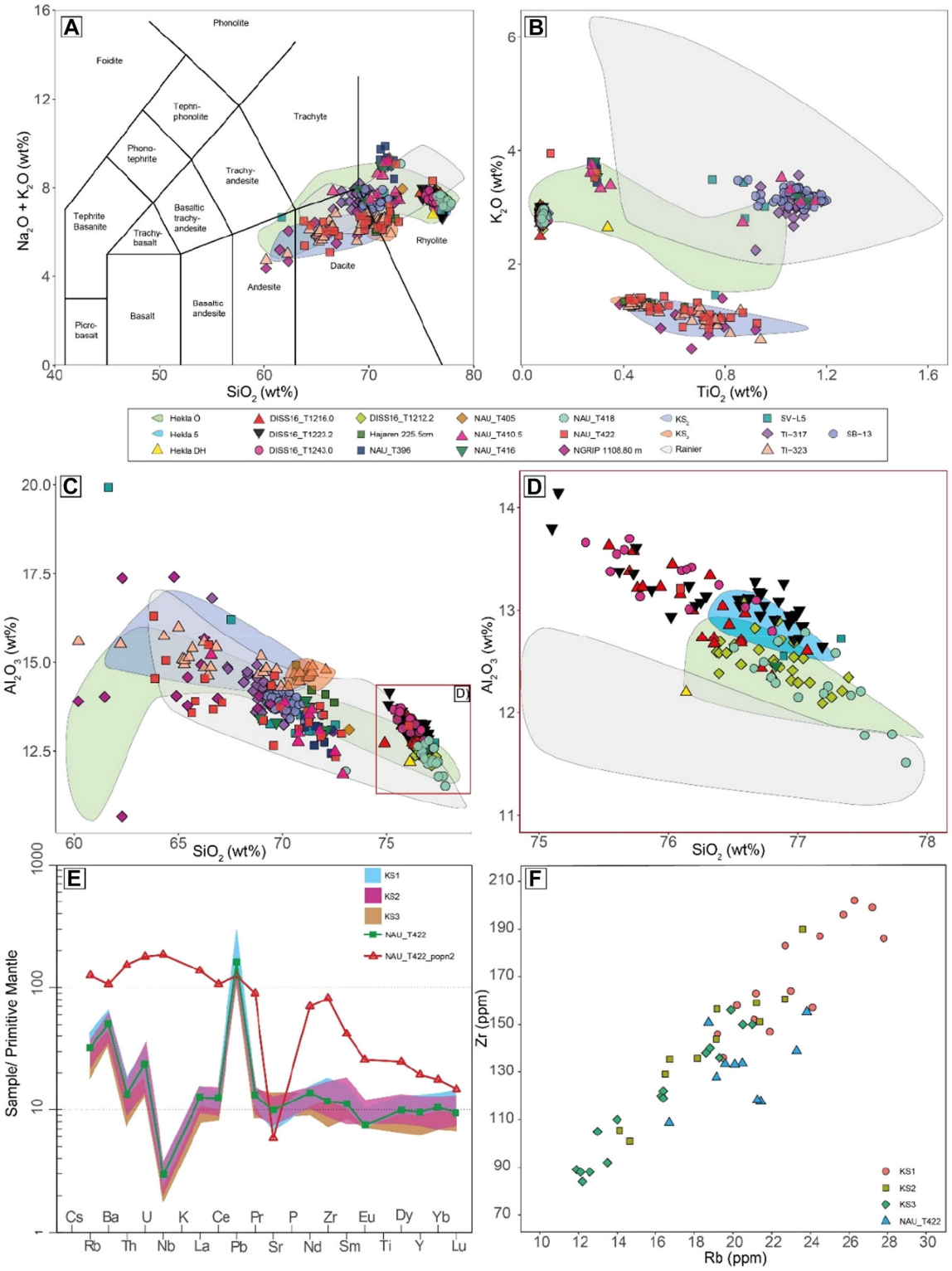

Figure 4. Major element geochemical plots for mid-Holocene target interval. For the biplots, only analyses with >60% were included (of the comparison tephras) for clarity of presentation. (A) TAS plot (Bas et al., 1986) including NAU_T396–NAU_T422 highlighting the range of andesites–rhyolites observed at Nautajärvi. (B) K_2O–TiO_2 plot showing Mount Rainier-type chemistry (Donoghue et al., 2007) and distal occurrences (Jensen et al., 2021). Several NAU23 layers also correspond to Katla-type chemistry, and those with the Hekla layers (Meara et al., 2020) plot distinctly with very low TiO_2. The low K_2O range of data corresponds to NAU_T422 and occurrences of the KS_2 layer from Ksudach. (C) There is a large spread in Al_2O_3 from KS_2, with the Hekla layers distinct in their high Al_2O_3 values for a given SiO_2. (D) Zoom-in of the Lairg A—additional Hekla layers identified within Diss Mere (Walsh et al., 2021, 2023). (E) Spider plot of trace elements from NAU_T422 and published KS_1, KS_2 and KS_3 chemistry, normalised to the primitive mantle (Portnyagin et al., 2020; Jensen et al., 2021). The red outlier is marked by the Katla-type shard found in NAU_T422. (F) Zr vs. Rb trace element plot, showing a potential enrichment in both elements over time, seen through lower values in the older KS_1 tephra and NAU_T422 sitting within the intermediate zone of KS_2. Care should be taken with this interpretation though, as trace elements were analysed on different machines, so may not be distinguishable outside of analytical errors. [Color figure can be viewed at wileyonlinelibrary.com]

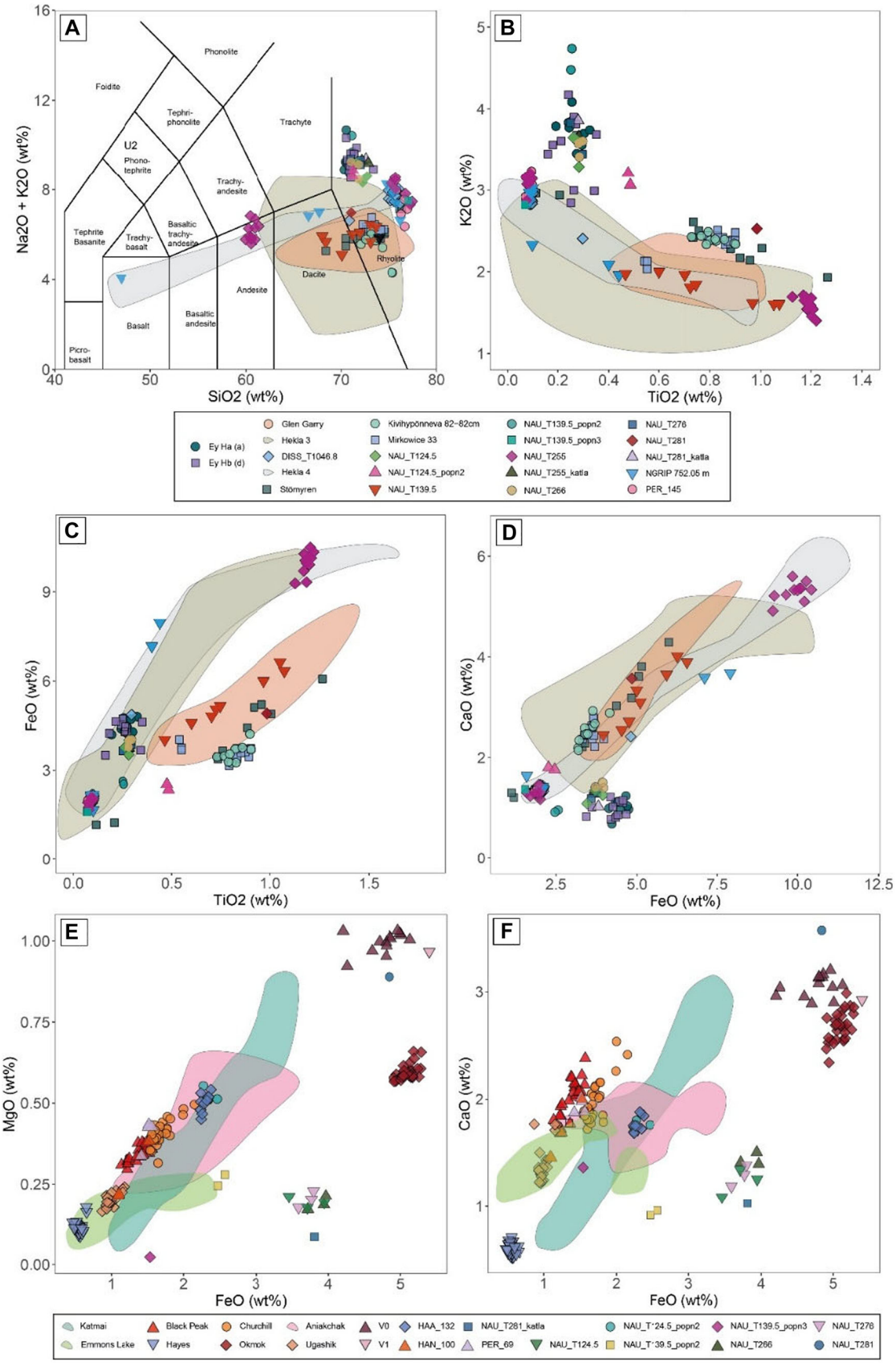

FIGURE 5 Continued.

tions (<30 shards/gram), which resulted in successful geochemical analysis from only NAU_T124.5 and NAU_T139.5. The ages of these layers based on the existing varve chronology of Ojala and Alenius (2005) are 1878 ± 20 varve yr BP and 2088 ± 20 varve yr BP, respectively. The peaks are rhyolitic, with variable SiO_2 values (~68–77 wt.%) and multiple chemical populations present within both layers.

The larger peak at NAU_T139.5 contains three distinct shard chemistries—the major population (NAU_T139.5_pop1) has seven analyses and spans the dacitic–rhyolitic boundary, with the total alkali content between 6 wt.% and 6.4 wt.%, with varying SiO_2 content (~68–74 wt.%). NAU_T139.5_pop1 is low-alkali and correlates well to Askja's alkali, FeO (3.32–8.02 wt.%) and TiO_2 (0.41–1.54 wt.%) values (Barber et al., 2008). There are several known eruptions of Askja within the late Holocene, the most widespread of which is the Glen Garry (GG) (Barber et al., 2008; Gudmundsdóttir et al., 2016; Kinder et al., 2020). Across northern Europe, another Askja eruption has been identified, the Stömyren, which is thought to be distinguishable from the GG on K_2O (Wastegård, 2005). The GG is generally <2.2 wt.% K_2O, while the Askja-like chemistries already identified in Finland (Kalliokoski et al., 2023) and Mirkowice, Poland, have higher K_2O and TiO_2 than the GG (Housley et al., 2014). Based on the closest match with the lower GG K_2O, NAU_T139.5 population one is correlated to this eruption of ~2000 Cal a BP.

Population two is rhyolitic and contains high K_2O values of ~4.6 wt.%, lower FeO and CaO than the main population of NAU_T139.5 as well as elevated alkalis that distinguishes it as broadly Torfajökull-type chemistry from southern Iceland (Meara et al., 2020). Torfajökull erupted several times within the Holocene (Plunkett and Pilcher, 2018; Walsh et al., 2021), with one candidate eruption only identified in the Swedish peat bog Gullbergbymossen and dated via linear interpolation of ^{14}C dates to be ~2600 Cal a BP, although with no GG was identified at this site (Wastegård, 2005). The analyses from NAU_T139.5 population two match well with the Gullbergby Tephra on major elements and so can be tentatively correlated to this tephra, which may be substantially (~600 years) younger than the ^{14}C dates from Gullbergbymossen indicate (Wastegård, 2005). The identification of just two shards with this chemistry within the same layer as the GG and without tephrostratigraphic investigations of the interval 2268–2800 Cal a BP means that reworking from the catchment cannot be ruled out.

Population two of NAU_T124.5 consists of two analyses that match Aniakchak-type chemistry from Alaska on all major elements excluding the alkalis (Fig. 5(E), (F)), which are slightly elevated (by <0.5 wt.%) in comparison with the Black Nose and Caldera Forming Eruptions (CFEs) of Aniakchak in the late Holocene (Bacon et al., 2014; Lubbers et al., 2024). The second major caldera-forming eruption of Aniakchak occurred in the late Holocene at ~3600 Cal a BP and produced a vast amount of volcanoclastic material (Miller and Smith, 1987; Blackford et al., 2014) reaching distal locations like Nordan's Pond in Newfoundland and Haapasuo in Finland (Pyne-O'donnell et al., 2012; Kalliokoski et al., 2023). The age of NAU_T124.5 (1878 ± 19 varve yr BP) is incongruous with these analyses correlating to a primary deposit of the Aniakchak CFE, but these shards may have been reworked from the catchment, after deposition of an Aniakchak CFE at 3600 Cal a BP: this is a somewhat long repose time for tephra to rework purely from the landscape.

There is some proximal evidence, however, of another, smaller Aniakchak eruption that may have occurred before or contemporary to the draining of a caldera lake that formed after the CFE—this has been dated indirectly to ~1800 Cal a BP, although tephra is absent from the proximal record, and the post-caldera geochemistry from whole-rock samples and lavas implies a shift towards slightly lower SiO_2 and K_2O (Bacon et al., 2014). Indeed, similar tephra geochemistry is identified for distal settings that post-date the Aniakchak CFE eruption (Kaufman et al., 2012), although this is substantially younger than the analyses identified here. Further investigation around the interval ~3600 Cal a BP in the Nautajärvi varves are necessary to assess whether these analyses could be reworked Aniakchak CFE, or indeed, whether they represent a younger eruption. Population one of NAU_T124.5 could not be correlated with any known source, although attempts are presented in the Supporting Information S1.

Discussion

Repeated Katla chemistry

Several Katla-sourced eruptions have been identified since 10 000 Cal a BP in Icelandic lakes, but these early- and mid-Holocene peaks contain basaltic chemistry, with none that match the rhyolitic chemistry seen in the Nautajärvi sequence (Gudmundsdóttir et al., 2016). The best known and used Katla-sourced tephra layer—the Vedde Ash—has been identified at >50 sites across Europe and the North Atlantic region and is a key marker of the mid Younger Dryas (Lane et al., 2012). One older eruption with identical chemistry has been identified in Norway and Scotland, termed the Dimnamyra, while two younger, early Holocene tephras have been identified distally with the same chemistry—the Abernethy (Matthews et al., 2011) and the Suduroy tephras (Wastegård, 2002). However, there is a shift in the geochemical signature of Katla eruptions in the mid-Holocene, with far-travelled Katla eruptions of the last ~6600 Cal a BP having substantially lower SiO_2 content (63–67 wt.%) and higher FeO and CaO, compared with the rhyolitic Katla eruptions prior to the Holocene (Larsen et al., 2001; Lane et al., 2012). The youngest reported Vedde Ash-type chemistry is thus dated to ~8200 Cal a BP, based on several bulk radiocarbon dates from Norway and the Faroes (Wastegård, 2002; Pilcher et al., 2005).

Investigations into multiple local early Holocene Katla-sourced layers from the Icelandic lake Torfadalsvatn contain

Figure 5. Geochemical plots for the Late Holocene interval from Nautajärvi. For the biplots, only analyses with >60% were included (of the comparison tephras) for clarity of presentation. (A) TAS plot (Bas et al., 1986) detailing the classifications of shards from this interval in Nautajärvi, as well as potential correlative eruptions. (B) K_2O–TiO_2 plot underlining the different K_2O values identifiable in the Stömyren and Glen Garry tephra layers (Dugmore et al., 1995; Wastegård, 2005; Watson et al., 2016; Wulf et al., 2016; Walsh et al., 2021). NAU_T139.5 is correlated to the lower K_2O Glen Garry eruption of Askja. Also distinct is the Hekla-type chemistry, with NAU_T255 overlapping with the low-TiO_2 Hekla 4 layer (Meara et al., 2020; Walsh et al., 2023; Davies et al., 2024). (C) FeO–TiO_2 plots further separate Glen Garry from the Stömyren instances, which include from Mirkowice and Kivihypönneva (Housley et al., 2014; Kalliokoski et al., 2023). Comparison with the Hekla 4 proximal chemistry (Meara et al., 2020) also matches well with NAU_T255. (D) FeO–CaO plots also highlight the good matches between Hekla 4 and NAU_T255, and Glen Garry with NAU_T139.5, while distinguishing the secondary populations of NAU_T139.5 and the Katla-type chemistry within NAU_T266, T276, T124.5 and T281 from Eyjafjallajökull-type chemistry of the Ey H(a) and (b) (Dugmore et al., 2013). (E) and (F) show comparisons of the minor populations of NAU_T139.5pop3, NAU_T281 and NAU_T124.5pop2 with North American comparisons from Bacon et al. (2014), Pearce et al. (2017) and Lubbers et al. (2024) as well as the distal occurrences from Kalliokoski et al. (2023). [Color figure can be viewed at wileyonlinelibrary.com]

very similar major element geochemistry to the Vedde Ash and it has been suggested that the layers in Torfadalsvatn can be distinguished based on higher FeO for a given TiO_2 compared with European instances of Vedde Ash composition (Lane et al., 2012; Harning et al., 2023). However, on examination of the rhyolitic standards for the European data used to compare the Vedde Ash chemistry with the Torfadalsvatn layers, the Loch Ashik FeO from Lane et al. (2012) is lower than the preferred values of the rhyolite StHs6-80G standard. For validation of the data, this chemistry has been substituted in Fig. 3(D) for another Scottish Vedde Ash occurrence from Lochan Feurach, which has FeO and TiO_2 values within the preferred range of the Lipari standard used (Kuehn et al., 2011; Carter-Champion et al., 2022). Normalised FeO versus TiO_2 chemistry shows that both the Torfadalsvatn Katla layers and indeed the multiple occurrences of Katla-type chemistry in the early Holocene found from the Nautajärvi sequence are indistinguishable from the Vedde Ash (Fig. 3(D)).

Whilst the Nautajärvi sediments are varved since 9625 varve yr BP (Ojala et al., 2005), there are several inflows to the lake, meaning that the potential for shards deposited in proglacial Lake Ancylus basin clay sediments prior to lake isolation may be stored in the Nautajärvi catchment deposits and transported into the lake basin during intervals of catchment erosion and redeposition during seasonal snow-melt events. Such a sustained concentration of Katla-type chemistry found consistently throughout the Holocene, even as recently as ~2000 varve yr BP, suggests a substantial deposition of an early Holocene or mid-Younger Dryas Katla-type chemistry onto the retreating ice sheet and proglacial landscape, but also storage in the catchment for thousands of years prior to their redeposition in Nautajärvi. Therefore, it is likely that these small peaks seen throughout the record represent slow and constant reworking of Vedde/Suduroy material from the surrounding landscape, rather than primary airfall from a different part of the magma chamber than has been seen from Katla in the late Holocene. However, this identification of reworked Katla-type chemistry should not affect the robustness of the isochrons identified from key target eruptions (Glen Garry, Hekla 4, Hekla 5/Lairg A and KS_2), as in each instance, the peaks are well resolved to 1 cm and there have been samples analysed below with no similar chemistry, indicating that the relevant peak corresponds to an isochron.

Long-term tephra reworking from the lake catchment in varved lakes is not an uncommon occurrence. Lane et al. (2015) found evidence of repeated Laacher See Tephra and Vedde Ash reworking throughout the Last Glacial Interglacial Transition and Holocene. These tephras correspond to a local volcanic eruption, recorded in the lake sediments as a visible tephra layer (>10 cm thick) and as a cryptotephra layer, respectively, highlighting the potential for tephra redeposition in varved lakes with limited catchments (Lane et al., 2015). However, at the time of these eruptions, Nautajärvi was first under the Fennoscandian Ice Sheet (FIS), which retreated at ~11 000 Cal a BP (Ojala and Alenius, 2005; Stroeven et al., 2016), and then part of the Baltic Sea basin during the Yoldia Sea and Lake Ancylus phases (Björck, 1995). To explain the repeated deposition of the Vedde Ash-type shards in Nautajärvi during the Holocene, we consider different scenarios including processes and depositional settings that might help to identify the sourced volcanic eruption.

Scenario 1: we might consider deposition of tephra onto the landscape when Nautajärvi was submerged under the Baltic Sea basin, which was then reworked from the catchment into lake basin. While it is a feasible option, there are no candidate eruptions of Katla with Vedde Ash-type chemistry after the retreat of ice from central Finland at ~11 000 Cal a BP and prior to ~8600 Cal a BP. The multiple early Holocene Katla eruptions detailed in Harning et al. (2023) occur between 11 460 and 11 200 Cal a BP and so would be deposited on top of the retreating ice sheet, presumably alongside the Vedde Ash that was deposited at ~12 100 Cal a BP (Lane et al., 2012; Stroeven et al., 2016). One further candidate would be the sparsely reported Suduroy tephra, which has an age estimate of <8310 Cal a BP (Pilcher et al., 2005; Wastegård, 2005). The largest peak of Katla-type chemistry is located at 8454 ± 85 varve yr BP but it also overlies smaller peaks of Katla chemistry, so it is unlikely that the Suduroy tephra could be the source of this high-concentration deposition of tephra over the Nautajärvi catchment, particularly as the varved nature of the sediments precludes downwards relocation of shards, as can be seen in Fig. 6.

Scenario 2: we might consider primary deposition of other Katla-like early Holocene tephra directly into Nautajärvi. Investigations into the Abernethy tephra identified in two Scottish lake sites that were formed at different points during the Younger Dryas found that the Abernethy was another eruption from Katla rather than merely reworked Vedde Ash because the lake had not formed at the time of the Vedde Ash eruption, but instead was under ice, precluding deposition of tephra into the lake at this time (MacLeod et al., 2015). Applying this logic to the Nautajärvi sequence is more challenging. It is likely that tephra from the Vedde Ash eruption was deposited on the FIS surface during late Weichselian deglaciation, and then transported into proglacial lake sediments due to ice sheet melting; however, during this eruption, the FIS margin was lying at the Salpausselkä zone ca. 100 km south of the lake Nautajärvi. It would be expected to find Vedde Ash particles in deposits of the Baltic Sea basin south of the Salpausselkäs, but more unlikely in areas so much further up ice (MacLeod et al., 2014).

As the Nautajärvi area was free of ice and under the Baltic Sea basin between ca. 11 000 and 9625 Cal a BP, one could expect to see small amounts of Katla-type tephra in the clastic component of the varves, as a result of one or multiple Katla eruptions, reworked from the landscape. This redeposition could have taken place in the early phases of lake evolution when colonisation of the emerging landscape by terrestrial vegetation was in the early phases and the catchment was more prone to terrain surface erosion. Perennial and semi-perennial snow cover have been shown to store tephra in large catchments for several hundred years (Davies et al., 2007), and a similar process could have occurred in the case of Nautajärvi. During the Early Holocene, the landscape surrounding Nautajärvi was more prone to surface erosion and seasonal snow melting provided large spring-time sediment inputs to the lake from the landscape (Ojala and Alenius, 2005), in a setting similar to that seen in Davies et al. (2007). As the landscape was stabilised by vegetation during the centuries following lake isolation, the widespread reworking of catchment detrital matter from previous glacial lake phases decreased, thus reducing the input of Katla-type shards into Nautajärvi lake basin, as seen in the varved Lake Kassjön, in Sweden (Petterson, 1999). The largest peak of Katla-type chemistry has a geochemical and temporal match with the Suduroy eruptions; however, it occurs close to a sequence of especially thick clastic varve laminae-sourced catchment erosion (Fig. 6). Therefore, at present, it is difficult to confidently assign this peak of 102 shards/g to either an isochronous tephra layer or reworked material (Fig. 3).

Scenario 3: An additional eruption of Katla in the early Holocene, post-isolation of Nautajärvi, which has not yet been characterised elsewhere, considering the growing body of work that suggests that Katla was highly active in the Early Holocene (Harning et al., 2023), is one of the more likely scenarios, based on the present information. However, scenario one cannot be fully ruled out at this point, as there is clearly sustained reworking of Vedde-type Katla chemistry throughout the

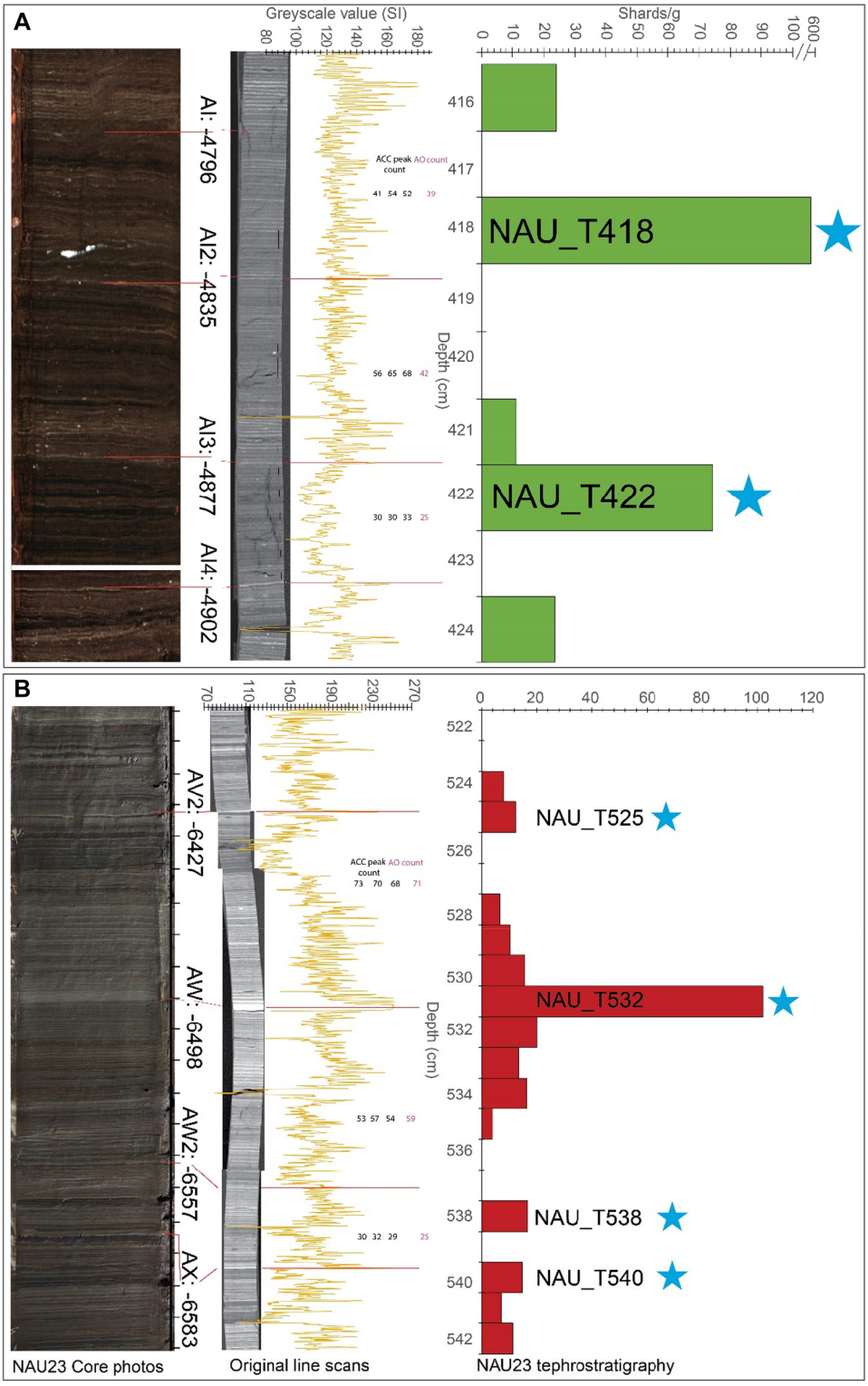

Figure 6. Comparison of core photos from the 2023 coring campaign with original line scan images from which the varve counts were produced. Greyscale values produced in ImageJ used to compare peak counting for (A) the interval between the deposition of NAU_T422 (KS_2 tephra) and NAU_T418 (Lairg A tephra) and (B) the peak of Katla chemistry at NAU_T532, highlighting the coincident peak in detrital material. [Color figure can be viewed at wileyonlinelibrary.com]

Holocene, even after a known shift in the chemistry of Katla, which means that the catchment of Nautajärvi can store tephra for hundreds and thousands of years.

Distal identification of mid-Holocene tephras and implications for age estimates

In the mid-Holocene, the tentative correlation of one population of NAU_T410.5 and NAU_T416 to Layers D or L from Mount Rainier is supported by identification of similar chemistry and attribution in several sites in eastern North America, as well as from Svartkälsjärn, Sweden (Watson et al., 2016; Jensen et al., 2021). However, there are temporal offsets between the Nautajärvi varve chronology (Ojala and Alenius, 2005) and the published non-varved sites. Layer D is calibrated in Donoghue et al. (2007) to be 6840 ± 70 Cal a BP, while Layer L is slightly older, at 7330 ± 60 Cal a BP. In Thin Ice Pond and Sydney Bog, there is a combined age estimate of 7215–6065 Cal

a BP, while in Sweden, the age is thought to be between 6500 and 6000 Cal a BP (Watson et al., 2016). In contrast, the Nautajärvi age estimate is 6726 ± 67 varve yr BP, which matches fairly well to Layer D, although neither layer D nor L estimates matches perfectly on the distally sourced layers. Further proximal geochemistry is required to confirm this correlation, although the match in both timing and chemistry is persuasive that tephra from Mount Rainier in North America reached lake Nautajärvi (Fig. 7).

This is not the only far-travelled tephra identified in the mid-Holocene at Nautajärvi; underlying the Lairg A peak is a low-K_2O rhyo-dacite that matches well to the caldera-forming KS_2 eruption from Ksudach volcano in Kamchatka (Braitseva et al., 1995, 1997; Kyle et al., 2011). While the KS_2 and slightly older KS_3 eruptions are chemically indistinguishable on major elements, the KS_2 eruption is generally accepted to be a larger eruption, with visible tephra deposits <900 km northward of Ksudach (Plunkett et al., 2015). Distal deposits of KS_2, confidently correlated and within expected time frames, have been identified in widely dispersed regions of Canada, Greenland ice-cores and Svalbard (Davies et al., 2016, 2024; van der Bilt et al., 2017; Jensen et al., 2021). The KS_3 has a more restricted dispersal supporting the assignment of NAU_T422 to the KS_2. This substantially extends the far-travelled component of this eruption to ~6700 km from source. Additionally, some evolution between KS_3 and KS_1 is evident when trace elements Zr and Rb are plotted, enabling more confident correlations between NAU_T422 and KS_2 (Fig. 4(F)). According to the Nautajärvi varve chronology, the KS_2 peak (NAU_T422) is dated at 6827 varve yr BP, 262 years younger than the Greenland Ice Core KS_2 age (7089 ± 26 Cal a BP). The centimetre in which KS_2 tephra is found in Nautajärvi is located a minimum of ~62 ± 1 varve years below the widespread Lairg A (NAU_T418) and 114 ± 6/9 varve years at maximum (counted three times to estimate uncertainty).

A minimum age for the Lairg A eruption is thus calculated using the Greenland Ice Core KS_2 age of 7089 ± 26 Cal a BP combined with counts of the varved 4-cm interval between the peaks of KS_2 and Lairg A (Fig. 6(A)): 62 ± 1 varves at minimum separate these 1 cm sampling intervals, meaning that the age of Lairg A must be younger than 7027 Cal a BP using this approach. At maximum distance between the two tephras (4 cm), the age of Lairg A is 6975 Cal a BP, with the counting error from multiple counts (18 years) added to the Greenland chronological uncertainty (26 years) and calculated as ±44 Cal a BP. Thus, the varve-based age estimate of the Lairg A is 7001 ± 44 Cal a BP. This is still outside of the 95% confidence interval for the Hekla-sourced tephra at T1212.2 (7166–7187 Cal a BP) in Diss Mere, which is correlated to the Lairg A (Walsh et al., 2021). It is also slightly older than the reported age of 6852–6947 Cal a BP from Plunkett and Pilcher (2018), although this is largely based on radiocarbon dating of non-laminated lake sediments, so is likely to be less precise than the age reported from the varved sediments of Diss Mere. Further support for this age estimate comes from the radiocarbon-based age of the Hekla 5/Lairg A at 7024 ± 134 Cal a BP identified in Kalliokoski et al. (2023). Although this shows an offset between the Nautajärvi varve chronology and calendar time that we discuss below, the identification of KS_2 and Lairg A/Hekla 5 within the same varved sequence allows validation of the timing between these two eruptions, that is, 88 years when comparing the KS_2 age from the Greenland ice-core chronology with Lairg A from the Diss Mere chronology, and 88 varve-years in the Nautajärvi chronology. This should also provide another means to distinguish between multiple Hekla eruptions in the early-mid Holocene. Walsh et al. (2023) identify five Hekla eruptions with very similar chemistry between ~8100 Cal a BP and ~6600 Cal a BP, and use additional eruptions of Torfajökull chemistry to aid identification of the different Hekla peaks: the identification of the KS_2 just prior to the deposition of the widespread Lairg A/Hekla 5 eruption should further aid distinguishing between these multiple Hekla eruptions.

The tentative identification of Azorean-type chemistry around ~7000 Cal a BP, based on a single shard, could serve as a distinguishing marker horizon if found in other sequences containing multiple Hekla peaks within this time frame. This shard is located *ca* 4 cm below the KS_2 layer, suggesting an approximate age of ~7150 varve yr BP. If the shard is indeed linked to the Furnas volcanic system, it would most likely originate from the Middle Furnas Group, although caution must be exercised at this stage, as there is just one analysis. However, there is considerably less reference glass material available for comparison with this minor population. While it is incredibly useful to have several tephras in common with the Greenland Ice Cores, the offset in the varve chronology from Nautajärvi and the ice-core annual layer counted Greenland record proves challenging and requires further discussion.

Consideration of the Nautajärvi chronology

The varve-based chronology of Nautajärvi is well established and has been used to examine several climatic shifts within the Holocene (Ojala et al., 2013, 2015; Lincoln et al., 2025). The robust continuous varve chronology of the Nautajärvi sequence (Ojala and Tiljander, 2003) enabled an independent assessment of the disadvantages of bulk radiocarbon dating in Boreal lakes where macrofossil-based ^{14}C dates are unobtainable and the lakes are seasonally hypoxic (Ojala et al., 2019). The identification of several well-dated tephra layers within this record allows for a separate assessment of the local reservoir effect at Nautajärvi: there is an existing ^{14}C date at the depth of the GG tephra layer that is offset by ~630 years. If this offset is applied consistently to the Nautajärvi ^{14}C dates and a P_Sequence is run in Oxcal, the local reservoir seems to be fairly consistent, with the additional tephra age estimates providing an indirect test of the potential variability of the local reservoir effect in Nautajärvi (Table 2 and Fig. 8(A)). This is fairly similar to the modern local reservoir effect measured from the near-bottom lake water at Valkiajärvi (Ojala et al., 2019) and suggests that perhaps local offsets in ^{14}C ages are more consistent than previously thought. It may be that this offset could be applied with some accuracy, providing either a modern assessment of the local reservoir effect is provided, or the tephra layers can be utilised to test the stationarity of the local reservoir back in time. However, the uncertainties associated with estimating a consistent local reservoir in this and other seasonally anoxic basins where in-lake processes are known to vary (Lincoln et al., 2025) preclude the use of bulk ^{14}C ages in the construction of any Nautajärvi age model in the future.

When the varve chronology is compared to the independent tephra age estimates (Table 3), the varve age estimate for GG matches well with independently established age controls from varved lakes Tiefer. See Żabińskie and Diss Mere, which also contain the GG (Wulf et al., 2016; Kinder et al., 2020; Martin-Puertas et al., 2021). However, further back in time, an offset emerges—the Hekla 4 Nautajärvi varve-based age estimate is 180 years younger than the Greenland Ice Core age, an offset beyond the estimated varve counting error of ±1%–2% (Ojala and Tiljander, 2003). Constraining more precisely the point at which the offset in ages begins in Nautajärvi is not possible at present, but through further tephra scans for the Aniakchak, OMH-185 or additional tephras found between 2000 and 4000 varve yr BP would help to pinpoint this divergence in chronologies. This offset is

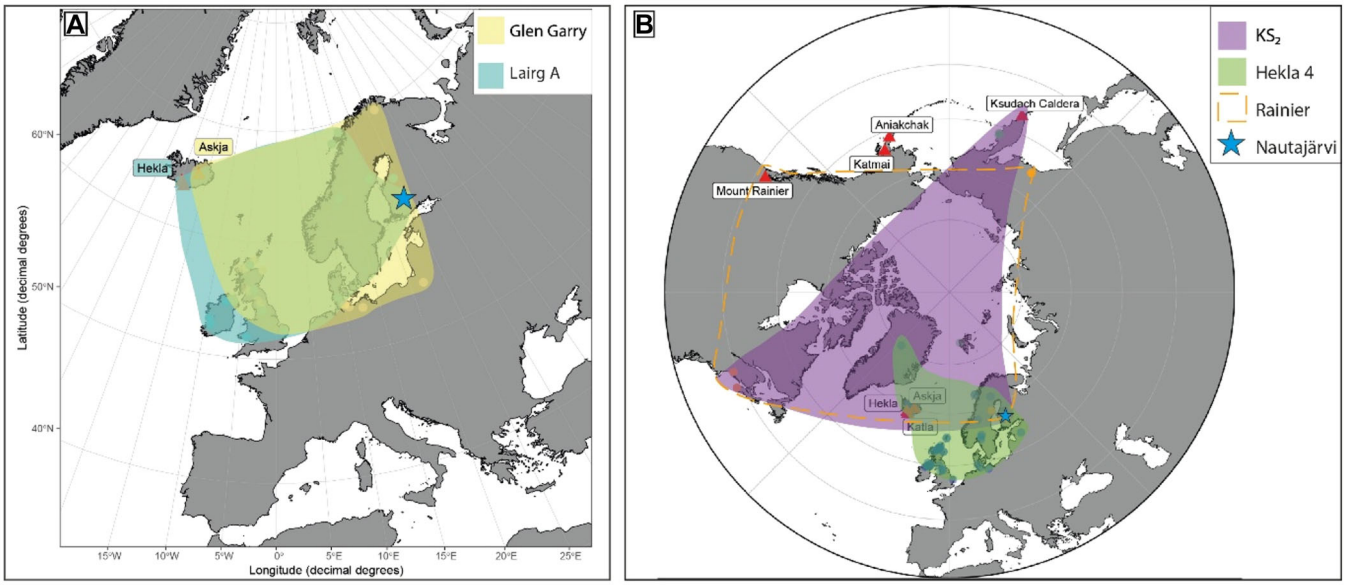

Figure 7. Updated distribution maps for relevant tephra layers found in Nautajärvi during the Holocene. (A) Icelandic sourced Glen Garry and Hekla 5/Lairg A eruptions showing that particularly in the case of Glen Garry, Nautajärvi represents the furthest NE occurrence of this eruption. (B) The KS_2 eruption is denoted by the purple shading, with Nautajärvi marked by the blue star, extending the known occurrence of this isochron from Greenland and Svalbard south to central Finland. In green shading is the widespread distribution of the Hekla 4 eruption, which was also recently found in the Greenland Ice Cores (Davies et al., 2024). The dashed orange line outlines the tentative correlation of Rainier type chemistry from the mid-Holocene, which has also been found in northeastern America, Alaska and Sweden (Watson et al., 2016; Jensen et al., 2021). For previously published occurrences of tephras, see the Supporting Information S1. [Color figure can be viewed at wileyonlinelibrary.com]

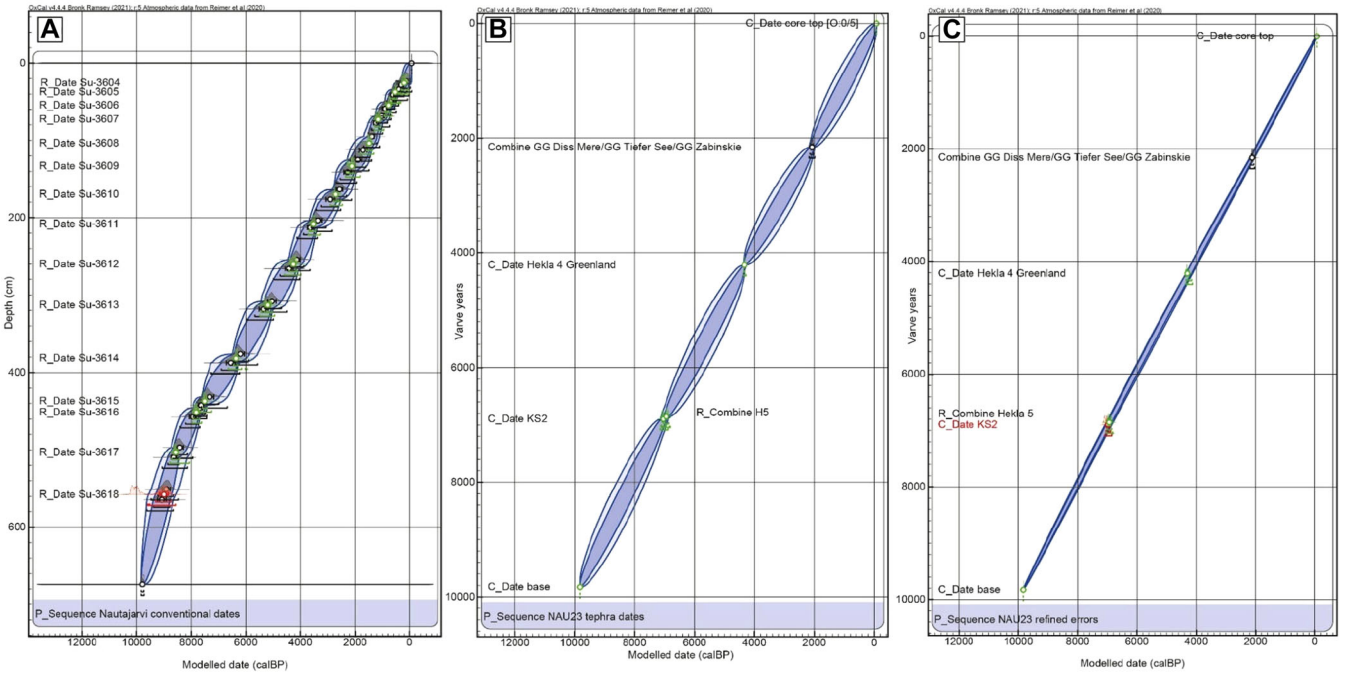

Figure 8. Age models for Nautajärvi. (A) This age model is constructed using the consistent reservoir offset based on the Glen Garry tephra layer paired with a radiocarbon date (Su-3609), as well as multiple embedded sequences to account for the large intervals that the radiocarbon dates were taken from. This model suggests that there may be some shift in sedimentation rate or the reservoir effect based on the change in the angle of the age model. (B) Using the numbers of varves estimated between each tephra intervals provides a more constrained approach to age modelling and results in a more linear model, albeit with larger errors than necessary perhaps. (C) Adopting the approach of Martin-Puertas et al. (2021), an inflexible K of 0.1 was used, as there should not be significant changes in sedimentation rate, as the varve formation at Nautajärvi was continuous and there were no large changes in varve thickness. However, this approach results in several outliers when the P_Sequence is run, notably being the independently corroborated Hekla 4 and KS_2 tephra age estimates, highlighting that there must be some missing varves or mismatch in the correlation of NAU-23 with the original Nautajärvi chronology. [Color figure can be viewed at wileyonlinelibrary.com]

exacerbated further back in time: at the deposition of Lairg A and KS_2 (which can be found within ~88 varve-years), where the difference between tephra age estimate and varve age estimate is 262 years. The identification of the KS_2 eruption in the Greenland Ice cores at 7089 ± 26 Cal a BP precludes any ambiguity in the location of this offset, and suggests that there must be further complexity in the varve chronology between ~4200 and 7000 Cal a BP.

This mid-Holocene interval is noted to contain higher proportional error in the original construction of the Nautajärvi

chronology (Ojala and Alenius, 2005): prior to ~4000 Cal a BP, the error estimate is approximately ±2 years per 200 years (10 years/ka), but this doubles to 4 years per 200 years between 4000 and 8000 Cal a BP. Even so, this offset is in excess of the estimated error within the varve chronology and results in clear issues when a P_Sequence is run using the varve chronology with reduced K value, an approach that was developed for the varved lake Diss Mere (Martin-Puertas et al., 2021). This model results in two outlier age estimates—the Hekla 4 and KS_2 from the Greenland Ice Cores—which are unlikely to be anomalous and instead highlight the potential for less varves to have been counted than exist. When the Nautajärvi age model is constructed using a variable K value to account for potential changes in sedimentation rate, as is utilised widely for non-laminated sediment records, no outliers are identified for the tephra age estimates (Fig. 8): moving forward, this offset of about 200 years that occurs between 2000 and 4000 Cal a BP between the Nautajärvi varve chronology and tephra chronology should be considered when high-resolution palaeoclimate and environmental interpretations are made from the Nautajärvi sequence using published varve-based age–depth models (e.g., Ojala and Alenius, 2005).

In order to account for this chronological offset, we consider several possibilities. The first is that the uncertainty in the Nautajärvi varve chronology is more extensive than has been reported before (e.g., Ojala and Tiljander, 2003; Ojala and Alenius, 2005). We note that there is good coherence of the GG tephra age between different records at around 2088 varve yr BP (Table 2), but below that, it seems that the number of varves in the Nautajärvi sequence may have been undercounted towards the mid- and early-Holocene. There is also an increased varve counting uncertainty found in the mid-Holocene, as reported by Ojala and Tiljander, (2003). The second potential source of the offset could be derived from a mis-correlation of individual marker layers when transferring the original Nautajärvi chronology to the new cores or potential contamination during coring and sediment sampling. The third possibility could relate to the integrity and temporal representation of the tephra isochrons in the Nautajärvi sequence. However, the presence of a systematic offset during this time undermines the potential for this option, and it might be expected that the tephras may be heterogeneous if they were the result of catchment input, particularly in the case of KS_2 and the Lairg A, which are separated by only 4-cm but contain high concentrations with no evidence of mixing between the two isochrons, which would be expected if they were deposited and remained on the landscape for 200 years post deposition.

A fourth possibility would be that the two unanalysed tephra at 430 and 441 cm are actually Hekla 5 and KS_2 as their varve-age chronologies are closer than the ages for these tephra and that the Hekla tephra that we have correlated to Hekla 4 is another unknown Hekla tephra that erupted 180 years later. This seems unlikely, however, as there would have to be three new unidentified tephra that happen to be in this record and no other, whereas the tephra that we have correlated to are well known in multiple records and show clear chemical correlations.

A final possibility may relate to the age estimates of the tephra layers within this offset period—however, as both Hekla 4 and the KS_2 eruptions are also identified within the well-constrained Greenland Ice Cores, and supported by independent dates from numerous other records, this is unlikely. As μXRF data are now available for the entire sequence (Lincoln et al., 2025), a more detailed assessment of the varves in this mid-Holocene interval will be conducted, with a particular focus on the composition of the detrital layers within the early-mid Holocene (Table 3).

Even considering this uncertainty within the mid-Holocene chronology for Nautajärvi, this record provides an excellent opportunity to explore how regional environmental shifts occurred within the Holocene for the sub-Arctic region, and through this tephrostratigraphy, it is possible to tie this high-resolution archive of Holocene climatic changes to records from across Europe and in Greenland. The varved nature of Nautajärvi and close coincidence of Lairg A and KS_2 enables a well-constrained age estimate for Lairg A that is at least 88 years (based on visual counts from high-resolution core images and μXRF analysis) younger than the deposition of the KS_2—this age estimate for Lairg A of 7001 ± 44 Cal a BP is robust and can be applied to less well-constrained records containing the Lairg A. Nautajärvi sits within the potential source areas of several volcanic systems, from Iceland, North America and Kamchatka, meaning that it offers the valuable opportunity to link with records from these regions to examine the timing of climatic shifts at a much broader scale than is normally possible. However, the tephrostratigraphic record is made more complicated by the persistent reworking of Katla-type rhyolites through the Holocene, likely from the slow release via snowpacks and the erosion of previous sediments from the Late Glacial, as well as the potential for missing varves within the mid-Holocene. Nonetheless, even with sustained reworking of Katla-type chemistry, ultra-distal tephras are identified within the Nautajärvi tephrostratigraphy, highlighting the value of investigating even small peaks in shard concentrations in varved lakes.

Conclusions

Nautajärvi contains 31 peaks in cryptotephra concentrations, with 18 of these yielding only Katla-type chemistry that are likely reworked and thus cannot be used as isochrons. Three peaks in tephra concentration could not be geochemically analysed, with the remaining 11 layers containing one or more geochemical populations that could be correlated to known volcanic systems or Holocene eruptions. The most notable of these is the high-concentration Lairg A/Hekla 5 peak, which is found across northern Europe and can be precisely dated to 7001 ± 44 Cal a BP using varve counting from the KS_2 peak

Table 3. Age offsets and estimates for Nautajärvi and published tephra layers. Diss tephra age from Martin Puertas et al. (2021), Hekla 4 and KS_2 from Davies et al. (2024) and Lairg A/Hekla 5 taken from this study.

Tephra	Varve age (varve yr BP)	Tephra age (Cal a BP)	Varve–tephra offset	Nautajärvi ^{14}C age (^{14}C a)	^{14}C Offset from varve yr BP	^{14}C–tephra age offset	Corrected ^{14}C age model (Cal a BP)
Glen Garry	2088 ± 21	2073 ± 39 (Diss)	−15	2980 ± 154	892	907	2239 ± 144
Hekla 4	4145 ± 41	4325 ± 8 (NGRIP)	180	4995 ± 160	850	670	4147 ± 132
Hekla 5/Lairg A	6762 ± 67	7001 ± 44 (this study)	239	7721 ± 201	959	544	7093 ± 202
KS_2	6827 ± 68	7089 ± 26 (NGRIP)	262	7778 ± 194	951	689	7164 ± 194
Suduroy	8459 ± 85		—	9028 ± 208	569	870	8789 ± 131

found in both Nautajärvi and the Greenland Ice Cores. The identification of both KS_2 and Hekla 4, which have also recently been identified within the Greenland Ice Cores, provides several absolute tie-points from which Greenland Holocene climate change can be compared in the future. Additionally, the location of the Glen Garry tephra also enables the comparison of Nautajärvi with the varved records Tiefer See (Germany), Żabińskie (Poland) and Diss Mere (England) for the late Holocene. Several more tentative tephra layers have been identified, sourced from more distal locations like the Furnas volcanic system in the Azores and potentially several North American volcanic systems like Mount Rainier. At present, due to the low numbers of analyses and presence within layers with heterogeneous chemical populations, these are only tentatively suggested but offer the potential for more widespread linkages of Nautajärvi to disparate Holocene records of environmental change.

Acknowledgements. This study was funded by the UKRI Medical Research Council through a Future Leaders Fellowship held by Celia Martin-Puertas, contributing to the research project DECADAL: Rethinking Palaeoclimatology for Society (MR/W009641/1). Antti Ojala was supported by Digital Waters Flagship (DIWA) (decision no. 359247) funded by the Research Council of Finland. The authors thank Saija Saarni and Emilia Kosonen, who helped with coring of Nautajärvi, as well as two anonymous reviewers, whose comments helped to improve the paper.

Data availability statement

The data that support the findings of this study are available in the supplementary material of this article.

Supporting information

Additional supporting information may be found in the online version of this article at the publisher's web-site.

NAU23 supplementary information.

NAU23 supplementary information2.

References

Andersen, K.K., Svensson, A., Johnsen, S.J., Rasmussen, S.O., Bigler, M., Röthlisberger, R. et al. (2006) The Greenland ice core chronology 2005, 15–42 ka. Part 1: constructing the time scale. *Quaternary Science Reviews*, 25(23–24), 3246–3257.

Andrén, T., Björck, S., Andrén, E., Conley, D., Zillén, L. & Anjar, J. (2011) The development of the Baltic Sea Basin during the last 130 ka. In: Harff, J., Björck, S. & Hoth, P. (Eds.) *The Baltic Sea Basin*. Berlin, Heidelberg: Springer, pp. 75–97.

Bacon, C.R., Neal, C.A., Miller, T.P., McGimsey, R.G. & Nye, C.J. (2014) *Postglacial eruptive history, geochemistry, and recent seismicity of Aniakchak volcano, Alaska Peninsula*. Reston, VA: U.S. Geological Survey.

Barber, K., Langdon, P. & Blundell, A. (2008) Dating the Glen Garry tephra: a widespread late-Holocene marker horizon in the peatlands of northern Britain. *The Holocene*, 18(1), 31–43.

Bas, M.J.L., Maitre, R.W.L., Streckeisen, A. & Zanettin, B. (1986) A chemical classification of volcanic rocks based on the total alkali-silica diagram. *Journal of Petrology*, 27(3), 745–750.

van der Bilt, W.G.M., Lane, C.S. & Bakke, J. (2017) Ultra-distal Kamchatkan ash on Arctic Svalbard: towards hemispheric cryptotephra correlation. *Quaternary Science Reviews*, 164, 230–235.

Björck, S. (1995) A review of the history of the Baltic Sea, 13.0–8.0 ka BP. *Quaternary international*, 27, 19–40.

Blackford, J.J., Payne, R.J., Heggen, M.P., de la Riva Caballero, A. & van der Plicht, J. (2014) Age and impacts of the caldera-forming Aniakchak II eruption in western Alaska. *Quaternary Research*, 82(1), 85–95.

Blockley, S.P.E., Pyne-O'Donnell, S.D.F., Lowe, J.J., Matthews, I.P., Stone, A., Pollard, A.M. et al. (2005) A new and less destructive laboratory procedure for the physical separation of distal glass tephra shards from sediments. *Quaternary Science Reviews*, 24(16–17), 1952–1960. Available from: https://doi.org/10.1016/j.quascirev.2004.12.008

Braitseva, O.A., Melekestsev, I.V., Ponomareva, V.V., Sulerzhitsky, L.D., Braitseva, O.A., Melekestsev, I.V. et al. (1995) Ages of calderas, large explosive craters and active volcanoes in the Kuril–Kamchatka region, Russia. *Bulletin of Volcanology*, 57, 383–402.

Braitseva, O.A., Ponomareva, V.V., Sulerzhitsky, L.D., Melekestsev, I.V. & Bailey, J. (1997) Holocene key-marker tephra layers in Kamchatka, Russia. *Quaternary research*, 47(2), 125–139.

Bronk Ramsey, C. (2008) Radiocarbon dating: revolutions in understanding. *Archaeometry*, 50(2), 249–275.

Bronk Ramsey, C. (2009) Bayesian analysis of radiocarbon dates. *Radiocarbon*, 51(1), 337–360.

Bronk Ramsey, C., Albert, P.G., Blockley, S.P.E., Hardiman, M., Housley, R.A., Lane, C.S. et al. (2015) Improved age estimates for key Late Quaternary European tephra horizons in the RESET lattice. *Quaternary Science Reviews*, 118, 18–32.

Carter-Champion, A., Abrook, A.M., Pike, J.H., Matthews, I.P., Palmer, A.P. & Lowe, J.J. (2022) Ice-sheet deglaciation and Loch Lomond Readvance in the eastern Cairngorms: implications of a Lateglacial sediment record from Glen Builg. *Journal of Quaternary Science*, 37(8), 1332–1347.

Chambers, F.M., Daniell, J.R.G., Hunt, J.B., Molloy, K. & O'Connell, M. (2004) Tephrostratigraphy of An Loch Mór, Inis Oírr, western Ireland: implications for Holocene tephrochronology in the north-eastern Atlantic region. *The Holocene*, 14(5), 703–720.

Davies, L.J., Jensen, B.J.L., Froese, D.G. & Wallace, K.L. (2016) Late Pleistocene and Holocene tephrostratigraphy of interior Alaska and Yukon: key beds and chronologies over the past 30,000 years. *Quaternary Science Reviews*, 146, 28–53.

Davies, S.M. (2015) Cryptotephras: the revolution in correlation and precision dating. *Journal of Quaternary Science*, 30(2), 114–130. Available from: https://doi.org/10.1002/jqs.2766

Davies, S.M., Albert, P.G., Bourne, A.J., Owen, S., Svensson, A. & Bolton, M.S.M. et al. (2024) Exploiting the Greenland volcanic ash repository to date caldera-forming eruptions and widespread isochrons during the Holocene. *Quaternary Science Reviews*, 334, 108707.

Davies, S.M., Elmquist, M., Bergman, J., Wohlfarth, B. & Hammarlund, D. (2007) Cryptotephra sedimentation processes within two lacustrine sequences from west central Sweden. *The Holocene*, 17(3), 319–330.

Donoghue, S.L., Vallance, J., Smith, I.E.M. & Stewart, R.B. (2007) Using geochemistry as a tool for correlating proximal andesitic tephra: case studies from Mt Rainier (USA) and Mt Ruapehu (New Zealand). *Journal of Quaternary Science*, 22(4), 395–410.

Dräger, N., Theuerkauf, M., Szeroczyńska, K., Wulf, S., Tjallingii, R., Plessen, B. et al. (2017) Varve microfacies and varve preservation record of climate change and human impact for the last 6000 years at Lake Tiefer See (NE Germany). *The Holocene*, 27(3), 450–464.

Dugmore, A.J., Cook, G.T., Shore, J.S., Newton, A.J., Edwards, K.J. & Larsen, G. (1995) Radiocarbon dating tephra layers in Britain and Iceland. *Radiocarbon*, 37(2), 379–388.

Dugmore, A.J., Newton, A.J., Smith, K.T. & Mairs, K.A. (2013) Tephrochronology and the late Holocene volcanic and flood history of Eyjafjallajökull, Iceland. *Journal of Quaternary Science*, 28(3), 237–247.

Gudmundsdóttir, E.R., Larsen, G., Björck, S., Ingólfsson, Ó. & Striberger, J. (2016) A new high-resolution Holocene tephra stratigraphy in eastern Iceland: improving the Icelandic and North Atlantic tephrochronology. *Quaternary Science Reviews*, 150, 234–249.

Guest, J.E., Gaspar, J.L., Cole, P.D., Queiroz, G., Duncan, A.M., Wallenstein, N. et al. (1999) Volcanic geology of Furnas Volcano, São Miguel, Azores. *Journal of Volcanology and Geothermal Research*, 92(1–2), 1–29.

Guest, J.E., Pacheco, J.M., Cole, P.D., Duncan, A.M., Wallenstein, N., Queiroz, G. et al. (2015) Chapter 9 The volcanic history of Furnas Volcano, São Miguel, Azores. *Geological Society, London, Memoirs*, 44(1), 125–134.

Harning, D.J., Thordarson, T., Geirsdóttir, Á., Miller, G.H. & Florian, C.R. (2023) Repeated Early Holocene eruptions of Katla, Iceland, limit the temporal resolution of the Vedde Ash. *Bulletin of Volcanology*, 86(1), 2.

Hayward, C. (2012) High spatial resolution electron probe microanalysis of tephras and melt inclusions without beam-induced chemical modification. *The Holocene*, 22(1), 119–125.

Heiri, O., Lotter, A.F. & Lemcke, G. (2001) Loss on ignition as a method for estimating organic and carbonate content in sediments: reproducibility and comparability of results. *Journal of Paleolimnology*, 25, 101–110.

Housley, R.A., MacLeod, A., Armitage, S.J., Kabaciński, J. & Gamble, C.S. (2014) The potential of cryptotephra and OSL dating for refining the chronology of open-air archaeological windblown sand sites: a case study from Mirkowice 33, northwest Poland. *Quaternary Geochronology*, 20, 99–108.

Jensen, B.J.L., Davies, L.J., Nolan, C., Pyne-O'Donnell, S., Monteath, A.J. & Ponomareva, V. (2021) A latest Pleistocene and Holocene composite tephrostratigraphic framework for northeastern North America. *Quaternary Science Reviews*, 272, 107242.

Johansson, H., Lind, E.M. & Wastegård, S. (2017) Compositions of glass in proximal tephras from eruptions in the Azores archipelago and their links with distal sites in Ireland. *Quaternary Geochronology*, 40, 120–128.

Jónsson, D.F., Gudmundsdóttir, E.R., Larsen, G., Óladóttir, B.A., Erlendsson, E., Eddudóttir, S.D. et al. (2020) The multi-component Hekla Ö Tephra, Iceland: a complex widespread mid-Holocene tephra layer. *Journal of Quaternary Science*, 35(3), 410–421.

Kalliokoski, M., Guðmundsdóttir, E.R. & Wastegård, S. (2020) Hekla 1947, 1845, 1510 and 1158 tephra in Finland: challenges of tracing tephra from moderate eruptions. *Journal of Quaternary Science*, 35(6), 803–816.

Kalliokoski, M., Guðmundsdóttir, E.R., Wastegård, S., Jokinen, S. & Saarinen, T. (2023) A Holocene tephrochronological framework for Finland. *Quaternary Science Reviews*, 312, 108173.

Kalliokoski, M., Wastegård, S. & Saarinen, T. (2019) Rhyolitic and dacitic component of the Askja 1875 tephra in southern and central Finland: first step towards a Finnish tephrochronology. *Journal of Quaternary Science*, 34(1), 29–39.

Kaufman, D.S., Jensen, B.J.L., Reyes, A.V., Schiff, C.J., Froese, D.G. & Pearce, N.J.G. (2012) Late Quaternary tephrostratigraphy, Ahklun Mountains, SW Alaska. *Journal of Quaternary Science*, 27(4), 344–359.

Kinder, M., Wulf, S., Appelt, O., Hardiman, M., Żarczyński, M. & Tylmann, W. (2020) Late-Holocene ultra-distal cryptotephra discoveries in varved sediments of Lake Żabińskie, NE Poland. *Journal of Volcanology and Geothermal Research*, 402, 106988.

Korkonen, S.T., Ojala, A.E.K., Kosonen, E. & Weckström, J. (2017) Seasonality of chrysophyte cyst and diatom assemblages in varved Lake Nautajärvi—implications for palaeolimnological studies. *Journal of Limnology*, 76(2), 366–379.

Kristjánsdóttir, G.B., Stoner, J.S., Jennings, A.E., Andrews, J.T. & Grönvold, K. (2007) Geochemistry of Holocene cryptotephras from the North Iceland Shelf (MD99-2269): intercalibration with radiocarbon and palaeomagnetic chronostratigraphies. *The Holocene*, 17(2), 155–176.

Kuehn, S.C., Froese, D.G. & Shane, P.A.R. (2011) The INTAV intercomparison of electron-beam microanalysis of glass by tephrochronology laboratories: results and recommendations. *Quaternary International*, 246(1–2), 19–47.

Kyle, P.R., Ponomareva, V.V. & Rourke Schluep, R. (2011) Geochemical characterization of marker tephra layers from major Holocene eruptions, Kamchatka Peninsula, Russia. *International Geology Review*, 53(9), 1059–1097. Available from: https://doi.org/10.1080/00206810903442162

Lane, C.S., Blockley, S.P.E., Mangerud, J., Smith, V.C., Lohne, Ø.S., Tomlinson, E.L. et al. (2012) Was the 12.1 ka Icelandic Vedde Ash one of a kind? *Quaternary Science Reviews*, 33, 87–99.

Lane, C.S., Brauer, A., Martín-Puertas, C., Blockley, S.P.E., Smith, V.C. & Tomlinson, E.L. (2015) The Late Quaternary tephrostratigraphy of annually laminated sediments from Meerfelder Maar, Germany. *Quaternary Science Reviews*, 122, 192–206.

Larsen, G., Newton, A.J., Dugmore, A.J. & Vilmundardóttir, E.G. (2001) Geochemistry, dispersal, volumes and chronology of Holocene silicic tephra layers from the Katla volcanic system, Iceland. *Journal of Quaternary Science*, 16(2), 119–132.

Lincoln, P., Tjallingii, R., Kosonen, E., Ojala, A., Abrook, A.M. & Martin-Puertas, C. (2025) Disruption of boreal lake circulation in response to mid-Holocene warmth; evidence from the varved sediments of Lake Nautajärvi, southern Finland. *Science of the Total Environment*, 964, 178519.

Lowe, D.J. (2011) Tephrochronology and its application: a review. *Quaternary Geochronology*, 6(2), 107–153.

Lubbers, J., Loewen, M.W., Wallace, K. & Coombs, M.L. (2024) *Source compositions of large tephra-production eruptions in Alaska*. Fairbanks, AK: Alaska Division of Geological & Geophysical Surveys.

MacLeod, A., Brunnberg, L., Wastegård, S., Hang, T. & Matthews, I.P. (2014) Lateglacial cryptotephra detected within clay varves in Östergötland, south-east Sweden. *Journal of Quaternary Science*, 29(7), 605–609.

MacLeod, A., Matthews, I.P., Lowe, J.J., Palmer, A.P. & Albert, P.G. (2015) A second tephra isochron for the Younger Dryas period in northern Europe: the Abernethy Tephra. *Quaternary Geochronology*, 28, 1–11.

Martin-Puertas, C., Walsh, A.A., Blockley, S.P.E., Harding, P., Biddulph, G.E. & Palmer, A. (2021) The first Holocene varve chronology for the UK: Based on the integration of varve counting, radiocarbon dating and tephrostratigraphy from Diss Mere (UK). *Quaternary Geochronology*, 61, 101134.

Matthews, I. & Pike, J. (2022) *AshplotR*. Egham, UK: Royal Holloway, University of London. Available at: https://doi.org/10.17637/rh.21941432.v1

Matthews, I.P., Birks, H.H., Bourne, A.J., Brooks, S.J., Lowe, J.J., MacLeod, A. et al. (2011) New age estimates and climatostratigraphic correlations for the Borrobol and Penifiler Tephras: evidence from Abernethy Forest, Scotland. *Journal of Quaternary Science*, 26(3), 247–252.

Meara, R.H., Thordarson, T., Pearce, N.J.G., Hayward, C. & Larsen, G. (2020) A catalogue of major and trace element data for Icelandic Holocene silicic tephra layers. *Journal of Quaternary Science*, 35(1–2), 122–142.

Miller, T.P. & Smith, R.L. (1987) Late Quaternary caldera-forming eruptions in the eastern Aleutian arc, Alaska. *Geology*, 15(5), 434–438.

Müller, W., Shelley, M., Miller, P. & Broude, S. (2009) Initial performance metrics of a new custom-designed ArF excimer LA-ICPMS system coupled to a two-volume laser-ablation cell. *Journal of Analytical Atomic Spectrometry*, 24(2), 209–214.

Ojala, A.E.K. & Alenius, T. (2005) 10 000 years of interannual sedimentation recorded in the Lake Nautajärvi (Finland) clastic–organic varves. *Palaeogeography, Palaeoclimatology, Palaeoecology*, 219(3–4), 285–302.

Ojala, A.E.K. & Saarinen, T. (2002) Palaeosecular variation of the Earth's magnetic field during the last 10 000 years based on the annually laminated sediment of Lake Nautäjarvi, central Finland. *The Holocene*, 12(4), 391–400.

Ojala, A.E.K. & Tiljander, M. (2003) Testing the fidelity of sediment chronology: comparison of varve and paleomagnetic results from Holocene lake sediments from central Finland. *Quaternary Science Reviews*, 22(15–17), 1787–1803.

Ojala, A.E.K., Heinsalu, A., Kauppila, T., Alenius, T. & Saarnisto, M. (2008) Characterizing changes in the sedimentary environment of a varved lake sediment record in southern central Finland around 8000 cal. yr BP. *Journal of Quaternary Science*, 23(8), 765–775.

Ojala, A.E.K., Heinsalu, A., Saarnisto, M. & Tiljander, M. (2005) Annually laminated sediments date the drainage of the Ancylus Lake and early Holocene shoreline displacement in central Finland. *Quaternary International*, 130(1), 63–73.

Ojala, A.E.K., Kosonen, E., Weckström, J., Korkonen, S. & Korhola, A. (2013) Seasonal formation of clastic-biogenic varves: the potential for palaeoenvironmental interpretations. *GFF*, 135(3–4), 237–247.

Ojala, A.E.K., Launonen, I., Holmström, L. & Tiljander, M. (2015) Effects of solar forcing and North Atlantic oscillation on the climate of continental Scandinavia during the Holocene. *Quaternary Science Reviews*, 112, 153–171.

Ojala, A.E.K., Saarnisto, M., Jugner, H., Snowball, I. & Muscheler, R. (2019) Biases in radiocarbon dating of organic fractions in sediments

from meromictic and seasonally hypoxic lakes. *Bulletin of the Geological Society of Finland*, 91(2), 221–235.
Pearce, C., Varhelyi, A., Wastegård, S., Muschitiello, F., Barrientos, N., O'Regan, M. et al. (2017) The 3.6 ka Aniakchak tephra in the Arctic Ocean: a constraint on the Holocene radiocarbon reservoir age in the Chukchi Sea. *Climate of the Past*, 13(4), 303–316. Available from: https://doi.org/10.5194/cp-13-303-2017
Petterson, G. (1999) Image analysis, varved lake sediments and climate reconstruction. Department of Ecology and Environmental Science, Umeå University, PhD Thesis, 17 pp.
Pilcher, J., Bradley, R., Francus, P. & Anderson, L. (2005) A Holocene tephra record from the Lofoten Islands, arctic Norway. *Boreas*, 34(2), 136–156.
Plunkett, G. & Pilcher, J.R. (2018) Defining the potential source region of volcanic ash in northwest Europe during the Mid-to Late Holocene. *Earth-Science Reviews*, 179, 20–37.
Plunkett, G., Coulter, S.E., Ponomareva, V.V., Blaauw, M., Klimaschewski, A. & Hammarlund, D. (2015) Distal tephrochronology in volcanic regions: challenges and insights from Kamchatkan lake sediments. *Global and Planetary Change*, 134, 26–40.
Ponomareva, V., Portnyagin, M., Pendea, I.F., Zelenin, E., Bourgeois, J., Pinegina, T. et al. (2017) A full Holocene tephrochronology for the Kamchatsky Peninsula region: applications from Kamchatka to North America. *Quaternary Science Reviews*, 168, 101–122.
Portnyagin, M.V., Ponomareva, V.V., Zelenin, E.A., Bazanova, L.I., Pevzner, M.M., Plechova, A.A. et al. (2020) TephraKam: geochemical database of glass compositions in tephra and welded tuffs from the Kamchatka volcanic arc (northwestern Pacific). *Earth System Science Data*, 12(1), 469–486.
Pyne-O'donnell, S.D.F., Hughes, P., Froese, D.G., Jensen, B., Kuehn, S.C., Mallon, G. et al. (2012) High-precision ultra-distal Holocene tephrochronology in North America. *Quaternary Science Reviews*, 52, 6–11.
Ramsey, C.B. & Lee, S. (2013) Recent and planned developments of the program OxCal. *Radiocarbon*, 55(2), 720–730.
Reimer, P.J., Austin, W.E.N., Bard, E., Bayliss, A., Blackwell, P.G., Bronk Ramsey, C. et al. (2020) The IntCal20 Northern Hemisphere radiocarbon age calibration curve (0–55 cal kBP). *Radiocarbon*, 62(4), 725–757.
Ruth Gudmundsdóttir, E., Larsen, G. & Eiríksson, J. (2011) Two new Icelandic tephra markers: The Hekla Ö tephra layer, 6060 cal. yr BP, and Hekla DH tephra layer, ~6650 cal. yr BP. land-sea correlation of mid-Holocene tephra markers. *The Holocene*, 21(4), 629–639.
Satow, C., Tomlinson, E.L., Grant, K.M., Albert, P.G., Smith, V.C., Manning, C.J. et al. (2015) A new contribution to the Late Quaternary tephrostratigraphy of the Mediterranean: Aegean Sea core LC21. *Quaternary Science Reviews*, 117, 96–112.
Sisson, T.W. & Vallance, J.W. (2009) Frequent eruptions of Mount Rainier over the last 2,600 years. *Bulletin of Volcanology*, 71, 595–618.
Stroeven, A.P., Hättestrand, C., Kleman, J., Heyman, J., Fabel, D., Fredin, O. et al. (2016) Deglaciation of fennoscandia. *Quaternary Science Reviews*, 147, 91–121.
Thorarinsson, S. (1971) The age of the light Hekla tephra layers according to corrected C14-datings. *Náttúrufræðingurinn*, 41, 99–105.
Tiljander, M., Ojala, A., Saarinen, T. & Snowball, I. (2002) Documentation of the physical properties of annually laminated (varved) sediments at a sub-annual to decadal resolution for environmental interpretation. *Quaternary International*, 88(1), 5–12.
Tomlinson, E.L., Thordarson, T., Müller, W., Thirlwall, M. & Menzies, M.A. (2010) Microanalysis of tephra by LA-ICP-MS—Strategies, advantages and limitations assessed using the Thorsmörk ignimbrite (Southern Iceland). *Chemical Geology*, 279(3–4), 73–89.
Turney, C.S.M. (1998) Extraction of rhyolitic component of Vedde microtephra from minerogenic lake sediments. *Journal of Paleolimnology*, 19, 199–206.
Walsh, A.A., Blockley, S.P.E., Milner, A.M. & Martin-Puertas, C. (2023) Updated age constraints on key tephra markers for NW Europe based on a high-precision varve lake chronology. *Quaternary Science Reviews*, 300, 107897.
Walsh, A.A., Blockley, S.P.E., Milner, A.M., Matthews, I.P. & Martin-Puertas, C. (2021) Complexities in European Holocene cryptotephra dispersal revealed in the annually laminated lake record of Diss Mere, East Anglia. *Quaternary Geochronology*, 66, 101213.
Wastegård, S. (2002) Early to middle Holocene silicic tephra horizons from the Katla volcanic system, Iceland: new results from the Faroe Islands. *Journal of Quaternary Science*, 17(8), 723–730.
Wastegård, S. (2005) Late Quaternary tephrochronology of Sweden: a review. *Quaternary International*, 130(1), 49–62.
Wastegård, S., Johansson, H. & Pacheco, J.M. (2019) New major element analyses of proximal tephras from the Azores and suggested correlations with cryptotephras in North-West Europe. *Journal of Quaternary Science*, 35, 114–121.
Watson, E.J., Swindles, G.T., Lawson, I.T. & Savov, I.P. (2016) Do peatlands or lakes provide the most comprehensive distal tephra records? *Quaternary Science Reviews*, 139, 110–128.
Wulf, S., Dräger, N., Ott, F., Serb, J., Appelt, O., Guðmundsdóttir, E. et al. (2016) Holocene tephrostratigraphy of varved sediment records from Lakes Tiefer See (NE Germany) and Czechowskie (N Poland). *Quaternary Science Reviews*, 132, 1–14.
Zillén, L.M., Wastegård, S. & Snowball, I.F. (2002) Calendar year ages of three mid-Holocene tephra layers identified in varved lake sediments in west central Sweden. *Quaternary Science Reviews*, 21(14–15), 1583–1591.